DOE/ER/40402--7

Nuclear Chemistry Progress Report

Oregon State University

W. LOVELAND

1 AUGUST, 1995 - 1 AUGUST, 1996

Table of Contents

I. Summary

In this report, we summarize the highlights of the week done between August 1, 1995, and August 1, 1996, that was supported by USDOE Grant No. DE-FG06-88ER40402. The work reported herein is the result of a collaborative effort between the nuclear chemists at Oregon State University and many other individuals and research groups. Each project discussed was the result of a joint effort of the groups, interchanging roles in data acquisition and analysis. The individuals contributing to each project are listed at the end of each section with the names of the Oregon State scientists underlined. Some of the work reported here is in its preliminary stages and use of the data contained in the preliminary reports should be made only after consultation with the appropriate authors. Up-to-date versions of many of these reports and new information can be found on our Web page at http://www.orst.edu/dept/nchem.

The work described is part of a project involving the study of low energy (<10 MeV/nucleon), and intermediate energy (10-100 MeV/nucleon) heavy ion reactions.

Our work in the low energy regime included:

- **the first U. S. studies of fusion utilizing radioactive beams.** We developed a method for using radioactive beams from the MSU A1200 PF facility, degrading them to near barrier energies and performing the measurements of the fusion excitation functions. Comparison of the fusion-fission excitation functions for the $^{32}S + ^{181}Ta$ reaction (measured at ATLAS) and the $^{38}S + ^{181}Ta$ excitation function show the predicted enhancement of the fusion probability below the fusion barrier and the lowering of the fusion barrier for the n-rich radioactive projectile relative to the stable projectile.

Half of our effort was spent in the study of intermediate energy nuclear collisions. Among the accomplishments were:

- **the establishment of a systematics of angular momentum transfer in peripheral collisions.** We found simple, apparently general correlations between transferred linear and angular momentum and between spin alignment and reaction Q-value in these reactions, in agreement with predictions of the nucleon transport model. Further tests of the robustness of this correlation were undertaken.

- **completion of the first portion of high resolution studies of heavy residue formation in reactions induced by 20 MeV/nucleon ^{197}Au utilizing the MSU A1200 separator.** The isotopically resolved velocity and yield distributions changed significantly when the target nucleus changed from ^{12}C to ^{27}Al to ^{nat}Ti. (The production of fusion-like residues declined while the role of dissipative phenomena increased.) Comparison of the data with predictions of incomplete fusion,

and nucleon transport models showed difficulties with each model.

- **synthesis of several new neutron-deficient nuclides in reactions of 20 MeV/nucleon ^{197}Au with heavy targets (Ti, Zr and Au).** At the current preliminary stage of the analysis, 48 new nuclides have been "identified."

- **our participation in exclusive studies of heavy residue formation in the reaction of 35 MeV/nucleon ^{86}Kr with ^{197}Au** in which it was found that the residues had large associated particle multiplicities indicating their formation in highly dissipative collisions, and that particle emission leading to residue formation relative to fission was favored as the dissipated energy increased.

II. Low Energy Heavy Ion Research

II. A. Fusion Enhancement with Radioactive Nuclear Beams

One of the interesting aspects of the study of nuclear reactions induced by radioactive beams is the possibility of using n-rich radioactive projectiles to synthesize new, neutron-rich heavy nuclei [1]. It has been shown [1] that new areas in the atomic physics and chemistry of the transactinide elements could be developed using intense n-rich radioactive beams.

Various authors [2-4] have suggested that there will be significant enhancements to the fusion cross sections for n-rich projectiles due to the lowering of the fusion barrier and the excitation of the soft dipole mode. They have further speculated that the use of these projectiles might lead to the successful synthesis of new or superheavy elements, a thought that has been echoed in the proposed Long Range Plan for Nuclear Physics. Several new radioactive beam facility proposals have focused, in part, on these possible attractive features of using n-rich radioactive beams. **The goal of this project is to make a measurement of the fusion enhancement factors for n-rich projectiles (of interest in the synthesis of new heavy nuclei).**

A readily available n-rich projectile that can act as a prototype for the projectiles likely to be involved in future heavy element synthesis is ^{38}S. (^{38}S ($t_{½}$ ~170 m) can be produced at the MSU A1200 radioactive beam facility by fragmentation of ^{40}Ar.) By measurement and comparison of fusion cross sections and excitation functions for the fusion of ^{32,34}S and ^{38}S with ^{181}Ta, we can evaluate quantitatively the expected fusion enhancement factors. ^{38}S (N/Z = 1.38) is as n-rich as any radioactive projectile nucleus available in reasonable intensities from radioactive beam facilities [5]. Comparison of its fusion properties with those of ^{32}S (N/Z = 1) should be a meaningful comparison. Specifically, ^{38}S can act as a prototype for the less available ^{54}Ca whose fusion enhancement factors have been calculated [4] and may provide impetus for more realistic calculations. Neither ^{32,38}S or ^{181}Ta are "magic" nuclei, and thus any special effects present in the fusion of shell stabilized nuclei will not be present. PACE calculations indicated that 99% of the compound nuclei formed in this reaction would fission so that the fusion-fission excitation functions should be equivalent to the fusion excitation function.

In runs in April, 1995 and March , 1996, we measured the fusion excitation function for the $^{38}S + ^{181}Ta$ reaction. A primary 40 MeV/nucleon ^{40}Ar beam was fragmented in a 120 mg/cm^2 Be production target in the A1200 fragment separator. After passage through an achromatic wedge, degrader, and momentum defining slits (to assure high beam purity) in the A1200, the beam was transported to the N3 area. The beam intensity was measured to be 2000-7000 ^{38}S/s on a 2x2 cm Ta target (with a primary Ar beam current of 15 pnA). The experimental apparatus used to measure the fusion cross sections is shown in Figure II-A-1. The ~8.5 MeV/nucleon ^{38}S beam was degraded to 150-260 MeV by an Al degrader that was remotely rotated to change its thickness. The energy straggling of the transmitted ions was about 15 MeV (FWHM) for degradation to 200 MeV. The degraded beam passed through a set of microchannel plate detectors and PPACs separated by 96 cm wherein the time of flight of the ions was measured. The time resolution of the MCP-MCP pair was measured to be 40 ps FWHM for an 8.5 MeV/nucleon ^{40}Ar beam (during the experiment). This time resolution allows measurement of the energy of each beam particle to within acceptable limits (<1 MeV). The efficiency of the "beam timing system" was measured to be 99.99%. Position sensitive PPACs mounted above and on either side of the Ta target detected prompt fission fragments, resulting from the de-excitation of the completely fused nuclei. (The efficiency of the PPACs for detecting fission fragments was typically >85%.) For tuning and measuring beam currents, a semiconductor detector was placed at 0° and at these low ^{38}S intensities the beam was allowed to strike it.

An energy spectrum of the radioactive beam taken with this silicon detector is shown in Figure II-A-2. The principal satellite on the beam is ^{35}Cl and it is clearly resolved from the ^{38}S. Silicon strip detectors or an array of surface barrier detectors mounted at backward angles detected any α-particles from the decay of evaporation residues that stop in the target or fission fragments. No residue decay α-particles were detected, giving further confidence in the assumption that all product nuclei fissioned. Folding angle distributions for the fission fragments were deduced from the coincident PPAC/strip signals. The differential fission cross sections, deduced from the PPAC and semiconductor signals, were fit with a $1/\sin\Theta$ distribution and integrated to yield the total fission cross sections. Absolute cross sections were determined by comparison with measurements of the known [7-8] fission cross section for the interaction of 115 and 149 MeV ^{16}O with ^{197}Au made with the same setup used during the March, 1986 run.

The resulting fusion-fission excitation function is shown in Figure II-A-3 along with a semi-empirical systematics of fusion excitation functions [6]. Looking at Figure II-A-3 (or its complement for the $^{32}S + ^{181}Ta$ system, Figure II-B-1) one sees evidence for enhanced fusion cross sections at sub-barrier energies for this system. Therefore, we fit the observed $^{38}S + ^{181}Ta$ excitation function with the coupled channels codes CCFUS and CCDEF[9] to reproduce this near barrier behavior (Figure II-A-4). We deduced a fusion barrier height of 130.7 ±2.0 MeV for the $^{38}S + ^{181}Ta$ reaction that is to be compared with a measured value of 137.5±1.0 MeV for the $^{32}S + ^{181}Ta$ reaction (section II-B). These values of the fusion barrier height agree with various systematics (Table II-A-1). From the point of view of synthesis of new heavy nuclei, this energy shift of about one neutron binding energy, can affect the production rates by factors of 10-1000.

It is interesting to test whether there is any evidence in this data for anything other than a

simple shift in the height of the fusion barrier as the projectile shifted from ^{32}S to ^{38}S. We show (Figure II-A-5) a reduced excitation function for the two systems. Within the uncertainties in the data, there is no evidence for any changes in excitation functions (barrier shape) in the two reactions. Finally we point out that the observed shift in the fusion barrier heights between the two reactions agrees with previous measurements and the expected lowering of the fusion barrier due to formation of a neck between the colliding nuclei [10].

With this understanding of the data in mind, we might speculate about their significance. It appears that the semi-empirical systematics of Gupta and Kailas[6] represents the new data adequately, if not conservatively (Figure II-A-3). Taking these systematics as an appropriate representation of the fusion enhancements that can be achieved with n-rich projectiles, we have evaluated some cases of current interest in heavy element synthesis. Using the formalism that has been shown to be of value in predicting heavy element synthesis reactions [1], we have the following heavy element production rates assuming fusion barriers from [6]:

Reaction	Predicted Production Rate (Atoms/Day)
$^{70}Zn + ^{208}Pb \rightarrow ^{277}112 + n$	6.
$^{70}Zn + ^{209}Bi \rightarrow ^{278}113 + n$	0.04
$^{44}S + ^{238}U \rightarrow ^{279}Hs + 3n$	0.6

The first reaction was used successfully at GSI to synthesize element 112[11] and the published cross section agrees quite well with this prediction made in July, 1995[12]. Based upon the results of this study, these attempts look quite promising. The last reaction represents the possible use of an ISL type facility to synthesize new n-rich nuclei (with $1 \leq t_{1/2} \leq 10$ s) for atomic physics and chemistry studies.

(K. E. Zyromski, W. Loveland, G. A. Souliotis, D. J. Morrissey, C. Powell, O. Batenkov, K. Aleklett, R. Yanez, M. Sanchez-Vega and I. Forsberg)

References

[1] W. Loveland, Proc. 3rd Int'l Conf. on Radioactive Nuclear Beams, D. J. Morrissey, ed. (Editions Frontieres, Gif-sur-Yvette, 1993), pp 526-536.

[2] N. Takigawa and H. Sagawa, Phys. Lett. **B265**, 23 (1991).

[3] M. S. Hussein, Nucl. Phys. **A531**, 192 (1991); Phys. Rev. **C44**, 446 (1991).

[4] C. H. Dasso and R. Donangelo, Phys. Lett. **B276**, 1 (1992); C. E. Aguilar, et al., Phys. Rev. C46, **R45** (1992).

[5] The Isospin Laboratory, LALP-91-51.

[6] S. K. Gupta and S. Kailas, Phys. Rev. **C26**, 747 (1982).

[7] T. Sikkeland, Phys. Rev. **135**, B669 (1960).

[8] V. E. Viola, Phys. Rev. **129**, 2710 (1963); T. Sikkeland, Phys. Rev. **125**, 1350 (1962).

[9] J. Fernandéz-Niello,C.H. Dasso, and S. Landowne, Comm. Phys. Comm. **54**, 409 (1989); C.H. Dasso, and s. Landowne, Comm. Phys. Comm. **46**, 187 (1987).

[10] C. E. Aguilar, V. C. Barbosa, L. F. Canto and R. Donangelo, Phys. Lett. **B201**, 22 (1988).
[11] S. Hofmann, et al., Z. Phys.(1996).
[12] K. Zyromski, et al., Nuclear Chemistry Progress Report, Oregon State University, 1995.

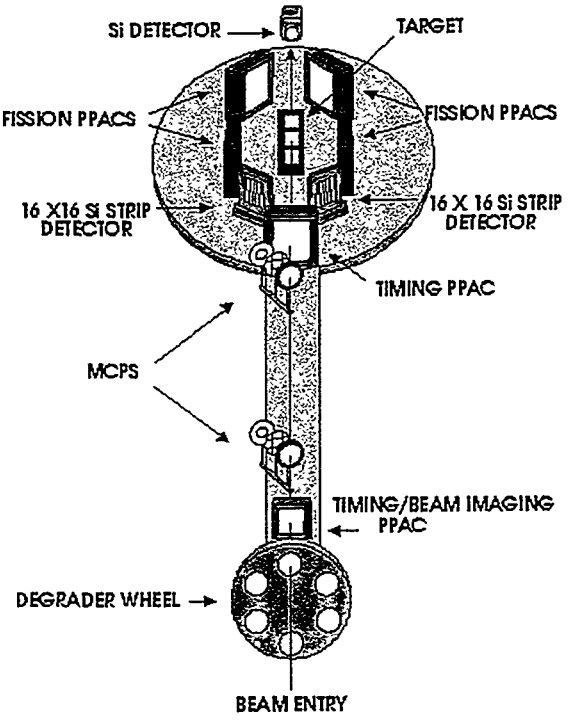

Figure II-A-1. Schematic diagram of experimental apparatus.

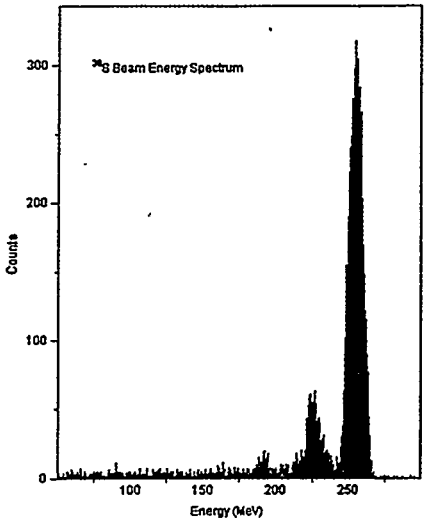

Figure II-A-2. Typical energy spectrum of the ^{38}S beam showing impurity levels.

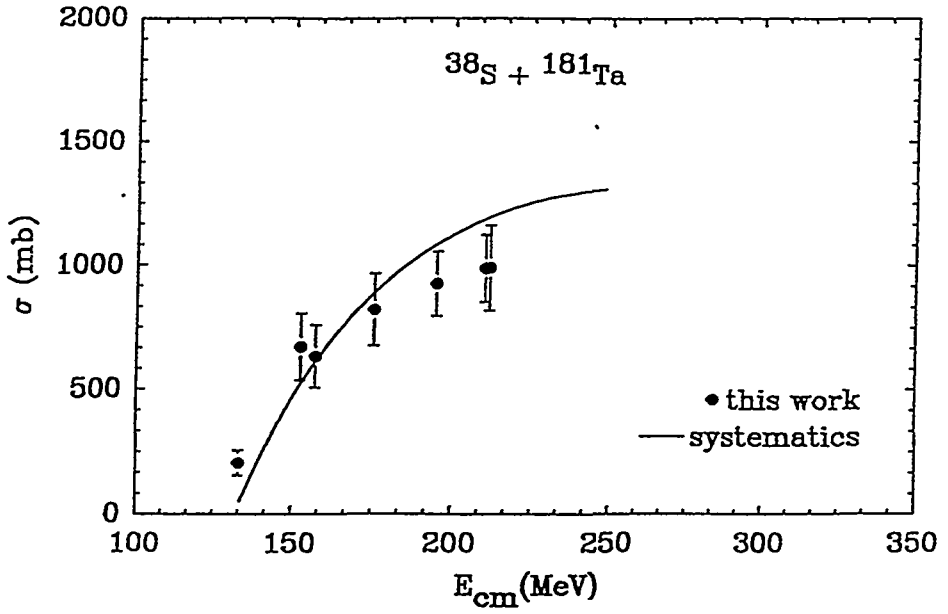

Figure II-A-3. Measured fusion-fission excitation function for the $^{38}S + ^{181}Ta$ reaction along with the semi-empirical systematics of Gupta and Kailas.

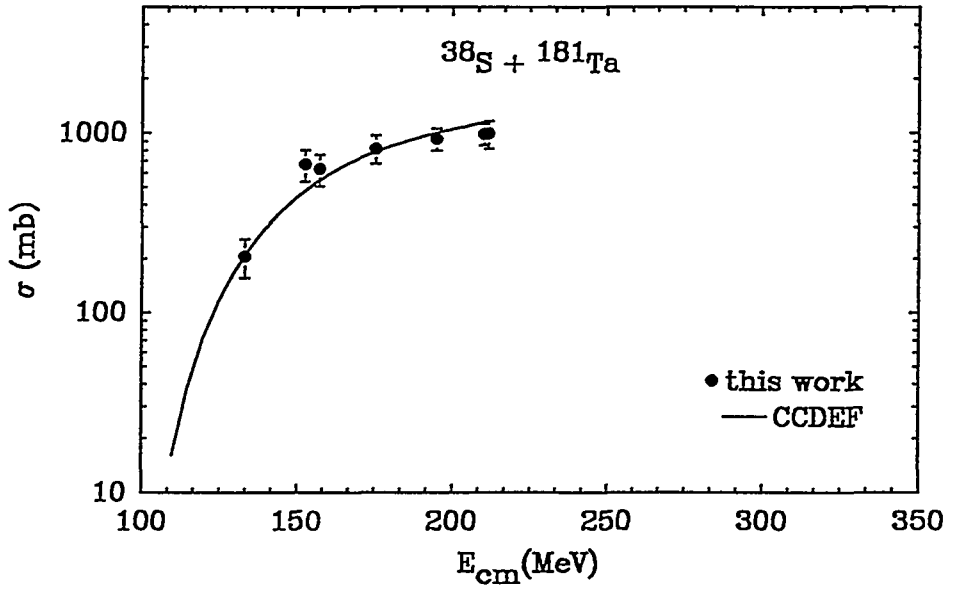

Figure II-A-4 Measured fusion-fission excitation function for the $^{38}S + ^{181}Ta$ reaction along with a coupled channels calculation for the same reaction.

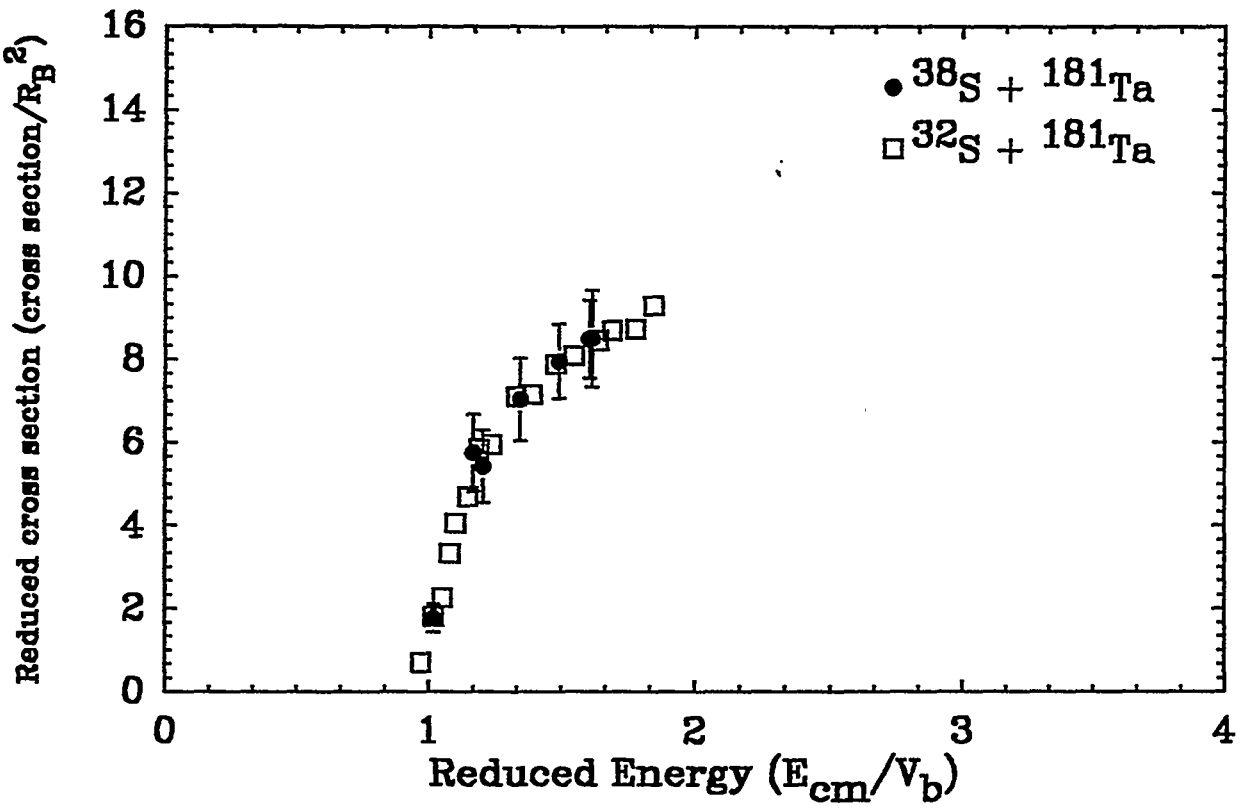

Figure II-A-5 Reduced excitation functions for the S + Ta reaction

II.B. Fusion-Fission Excitation Function for the $^{32}S + ^{181}Ta$ Reaction

As part of our study of fusion enhancement with neutron-rich radioactive beams, we needed to compare the fusion-fission excitation function for the $^{38}S + ^{181}Ta$ reaction with the $^{32}S + ^{181}Ta$ excitation function. Since the latter reaction has not been studied, we used the ATLAS accelerator facility to make this measurement.

Well-focussed, collimated ^{32}S beams of well-defined energy (typical energy spread = 0.2 MeV) from ATLAS struck a 0.46 mg/cm^2 Ta target mounted in the center of the 36" scattering chamber. An array of 16 silicon surface barrier detectors (300 mm^2) were used to detect the coincident fission fragments from this reaction emerging at angles from 15° to 160°. Cross section measurements were made at sixteen ^{32}S energies between 150 and 300 MeV. At each energy, the measured fragment angular distributions were transformed into the center of mass, fit with a $1/\sin\theta$ distribution and integrated to give the total fission cross section. (No significant differences in deduced total fission cross sections resulted when a more exact [1] form of the fragment angular distribution was used.) The absolute magnitude of the cross sections was determined by normalizing the observed elastic scattering cross section in the forward detectors to the Rutherford scattering cross section. The resulting fusion-fission excitation function is shown in Figure II-B-1 and Table II-B-1.

The compound nucleus is ^{213}At, formed at excitation energies of 47-174 MeV. According to PACE [2] simulations with a value of $a_f/a_n = 1.00$[3] and temperature dependent values of a [5], the fraction of the reactions that leads to fission is 0.99 and it does not change appreciably with projectile energy. Furthermore, in the related study of $^{38}S + ^{181}Ta$ reaction, no evaporation residues were observed even though their abundance was expected to be larger. Therefore we have taken the fusion-fission excitation function to be the fusion excitation function for this reaction.

Because of our desire to compare these data with the less well known data from the $^{38}S + ^{181}Ta$ reaction, we have made a simple analysis of the data which can be applied in both reactions. We have performed a simple coupled channels calculation using the codes CCFUS and CCDEF [6]. In the coupled channels calculation, we have included the deformation of the target nucleus [7], the excitation of the first quadrupole and octupole states of projectile (with B(E2) and B(E3) values from [8] and [9]), and the excitation of the low-lying states of the ground state rotational band of ^{181}Ta (B values from [10]). The strength of the nuclear potential was varied to give the best overall fit to the experimental data, giving $V_b = 137.5$ MeV. The resulting fit to the data is shown in Figure II-B-1 along with semi-empirical predictions of the fusion excitation function for this reaction [4,11]. The predicted values of the one-dimensional fusion barrier height are similar but the parameterization of the fusion cross section differs. The better fit of the coupled channel calculations below the fusion barrier shows the importance of sub-barrier fusion enhancement in this system.

In Table II-B-2, we show a comparison of the deduced values of the strength of the nuclear potential with various empirical predictions of these quantities. The best overall agreement with our measurements is with the estimates of ref [11], especially if we consider the magnitude of the fusion cross section above the barrier. However, none of these one-dimensional empirical prescriptions works very well in predicting the sub-barrier fusion

enhancement.

(K. E. Zyromski, W. Loveland, G. A. Souliotis, J. R. Dunn and B. G. Glagola)

References

1. R. Vandenbosch and J. R. Huizenga, Nuclear Fission (Academic, New York, 1973) p 183.
2. A. Gavron, Phys. Rev. **C21**, 230 (1980).
3. Th. Rubehn, K.X. Jing, L.G. Moretto, L. Phair, K. Tso, and G.J. Wozniak, LBNL-38865..
4. W. W. Wilcke, et al., At. Data and Nuclear Data Tables **25**, 391 (1980).
5. S. Schlomo and J. B. Natowitz, Phys. Rev. **C44**, 2878 (1991).
6. J. Fernandez -Niello, C. Dasso, and S. Tandowne, Com. Phys. Comm. **54**, 409 (1989).
7. P. Möller, J.R. Nix, W.D. Myers, and W.J. Swiatecki, At. Data and Nucl. Data Tables **59**, 185 (1995).
8. S. Raman, C. Malarkey, W. Milner, C. Nestor, Jr. and P. Stetson, At. Data and Nucl. Data Tables **36**, 1 (1987).
9. R. H. Spear, At. Data and Nucl. Data Tables **42**, 55 (1989).
10. W. Andrejtschuff, K. D. Schilling and P. Mantrass, At. Data and Nucl. Data Tables **16**, 515 (1975).
11. S.K. Gupta and S. Kailas, Phys. Rev **C26**, 747 (1982).

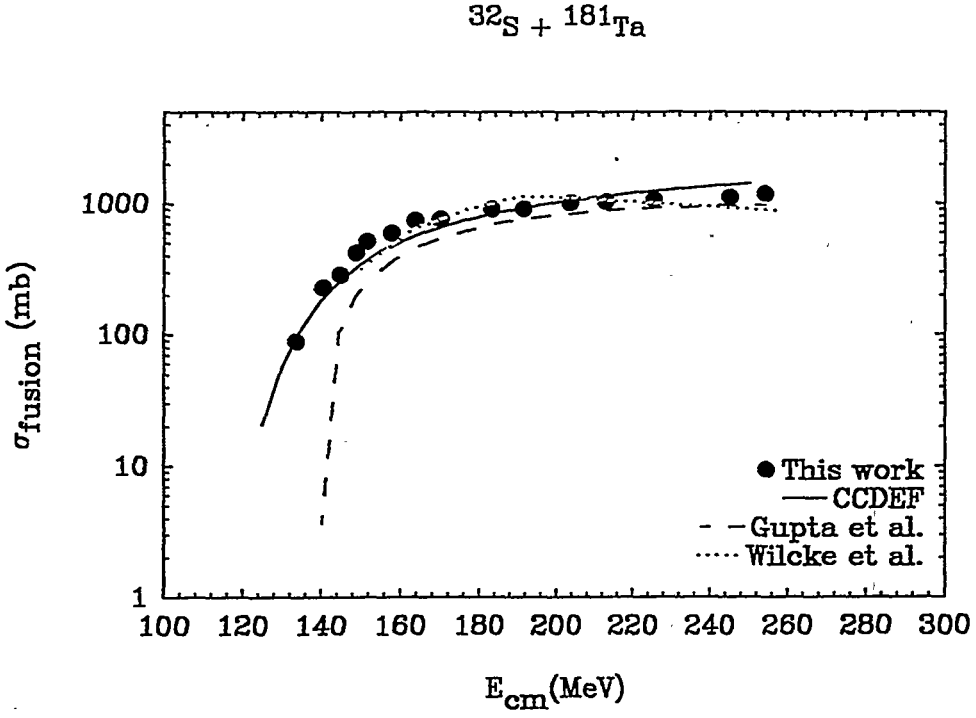

Figure II-B-1. Fusion excitation function for the $^{32}S + ^{181}Ta$ reaction.

Table II-B-1
Fusion-Fission Excitation Function Data

^{32}S Energy (MeV)	σ_{fiss} (mb)
299.1	1180 ± 23
288.3	1108 ± 5
274.3	1104 ± 21
265.5	1074 ± 20
250.6	1028 ± 20
239.6	1002 ± 10
225.3	910 ± 18
215.6	904 ± 12
200.1	757 ± 15
192.4	743 ± 19
185.6	597 ± 17
178.3	515 ± 25
175.1	423 ± 8
170.2	287 ± 7
165.1	230± 4
157.3	88.6 ± 4.0

Table II-B-2

Fusion Barriers for the
S +Ta reaction

Source	V_b(MeV)
This work	137.5±1.3
Gupta and Kailas[11]	139.7
Wilcke, et al.[4]	137.9
Bass[12]	137.0

III. Intermediate Energy Heavy Ion Research

III.A. Systematics of Angular Momentum Transfer in Intermediate Energy Nuclear Collisions

In heavy-ion collisions, large angular momenta can be transferred to an intermediate complex through the dissipation of the incoming orbital angular momentum. The magnitude of the transferred angular momentum and its alignment can be determined by measuring the angular distributions of sequentially emitted fission fragments, light particles or γ-rays [1-8]. At intermediate energies (from 10 to 100 MeV/nucleon) the linear momentum transfer has been shown to play an important role in determining the evolution of reaction mechanisms and in demonstrating the transitional character of this regime between mean field behavior at low energies and the dominance of nucleon-nucleon interactions at high energies [9]. In the intermediate regime, the systematic behavior of linear momentum transfer has been extensively studied mainly through measurements of the correlation angle between fission fragments [9]. Several studies have shown a correlation between transferred linear and angular momenta for some systems at intermediate energies. However, the systematic behavior of angular momentum transfer in intermediate energy reactions has not yet been established.

In this article, we report a measurement of the fission fragment angular distributions, both in and out of the reaction plane, in coincidence with projectile-like fragments from which the transferred angular and linear momentum can be inferred for the reaction of 22 and 30 MeV/nucleon ^{16}O with ^{197}Au. By combining these measurements with existing data, an unexpected simple universal correlation between transferred linear and angular momentum in intermediate energy nuclear collisions was observed.

During the past year, we have modified and improved the analysis of these data and their interpretation. For the convenience of the reader, we include (in this article) some material that was reported previously [23] so that a complete story is presented rather than the developments of the past year. A paper summarizing this information has been published [24].

The experimental arrangement was similar to that used in ref [3-5, 8]. Beams of 357 and 476 MeV ^{16}O from the Gustav Werner cyclotron in Uppsala were incident on a self-supporting 325 $\mu g/cm^2$ thick Au target. Fission fragments (F) were detected in-and out-of the reaction plane in coincidence with projectile-like fragments (PLFs). PLFs were identified using a three element (200, 1000, and 5000 μm) semiconductor detector telescope placed at 20° (357 MeV) or 15° (476 MeV), close enough to the grazing angles (15°, 11°, respectively) to insure adequate PLF yields. The beam axis and the vector between the target and the PLF telescope defined what we will call the "reaction plane." The fission fragments were detected by an array of twelve surface barrier detectors (9 in-plane and 3 out-of-plane) that was moved as a unit to different angles. The detected events were of two types: (a) a PLF-F coincidence involving a PLF and a fission fragment detected whether in-plane or out-of-plane; or (b) a PLF-F-F coincidence in which all three fragments were detected in the reaction plane.

To establish the linear momentum transfer in a relatively model-independent way, we

used the triple coincidence data, i.e., the PLF-F-F events. We assumed that the exit channel involved more than the three detected particles, i.e., we did not assume "massive transfer" or two body kinematics. Instead we assumed that the exit channel involved some "missing mass", M_m with an associated momentum P_m. Following the procedure of Back et al., [10,11] we deduced a linear correlation between the parallel component of the observed momentum of the PLF, $P_3^{\parallel}$ and the parallel component of the momentum of the recoiling nucleus before fission, $P_R^{\parallel}$. The correlation observed between $P_3^{\parallel}$ and $P_R^{\parallel}$ was similar for the reactions of 20 MeV/nucleon ^{16}O with ^{238}U [10] and 22 MeV/nucleon ^{16}O with ^{197}Au. The average missing momentum deduced in this analysis was substantial, indicating the need for this type of analysis. The deduced missing momentum is used explicitly in the calculation of Q values and implicitly in the deduction of $P_R^{\parallel}$ using the $P_3^{\parallel}/P_R^{\parallel}$ correlation Expressed as fractional linear momentum transfer (FLMT), the missing momentum was 0.24 and 0.31 in the 22 and 30 MeV/nucleon-induced reactions, respectively.

To analyze the coincidence events where only one fission fragment is detected, the parallel recoil momentum was assumed to follow the relationship between $P_3^{\parallel}$ and $P_R^{\parallel}$ established from the PLF-F-F coincidences and its perpendicular component was assumed to be equal in magnitude to the perpendicular momentum component of the PLF. (The deduced value of $P_R^{\parallel}$ has been shown [10] to be insensitive to this latter assumption.) The measured events were transformed into the rest-frame of the recoil on an event-by-event basis. The resulting angular distributions were sorted into three bins based on reaction Q-value, where -Q was taken as $E_{proj} - E_3 - E_R - E_m$. The mean fission fragment kinetic energies in the moving frame agree with systematics [12] for the fission of Au. The angular distributions are shown in Figure III-A-1.

The angular correlations observed in the sequential fission fragment angular distributions are treated within a statistical model where the production of the in-plane components arises from the thermal excitation of angular momentum bearing collective modes [13]. The statistical excitation of the above modes leads to Gaussian distributions of the components of the spin of the fissioning nucleus, where the only nonzero average component lies along the quantization axis,

$$P(I) = exp\left\{-\left[\frac{I_x^2}{2\sigma_x^2} + \frac{I_y^2}{2\sigma_y^2} + \frac{(I_z - \langle I_z \rangle)^2}{2\sigma_z^2}\right]\right\} \qquad (1)$$

The angular distribution of the fission fragments in the rest frame of the fissioning nucleus is given by [14],

$$W(\theta,\phi) = \frac{1}{S} exp\left[-\frac{1}{2}\left(\frac{\langle I_z \rangle \cos\theta}{S}\right)^2\right] \qquad (2)$$

where

$$S^2 = K_0^2 + (\sigma_x^2 \sin^2\phi + \sigma_y^2 \cos^2\phi)\sin^2\theta + \sigma_z^2 \cos^2\theta \qquad (3)$$

These equations ((2) and (3)) represent a frequently used approximation [3,5,8,13] to the more exact quantum mechanical calculation[20]. This approximation is believed to be good except for the region where $\theta=0°$. K_0^2 is the mean square projection of the total angular momentum I along the nuclear symmetry axis of the fissioning nucleus at the saddle point. We have estimated K_0^2

by scaling the value appropriate for U- like nuclei to the present system(Au-like nuclei [15]), using the ratio of the moments of inertia at the saddle point derived from the liquid drop model [21].

To extract the transferred angular momentum $J=\langle I_z \rangle$, and degree of alignment P_{zz}, defined as

$$P_{zz} = \frac{3}{2} \frac{\left\langle \langle I_z \rangle^2 \right\rangle}{\langle I^2 \rangle} - \frac{1}{2} \qquad (4)$$

from the measured data, we have fit the measured distributions using equations (2) and (3). We have assumed that $\sigma_y = 0$[22]. The direction of the separation axis, χ, has been included explicitly as an additional parameter by replacing ϕ by $\phi+\chi$ in the prescription for $W(\theta, \phi)$. (The separation axis of the fissioning system need not correspond to the recoil axis.) The parameters resulting from fitting the measured in-plane and out-of-plane angular distributions are given in Table III-A-1 and the calculated angular distributions shown as solid lines in Figure III-A-1. (The uncertainties in $\langle I_z \rangle$ reflect only the uncertainties due to the chi-square minimization and the finite size of each Q bin, and not any uncertainties due to the analysis.) The "best fit" values of the shift angles, χ, are substantially smaller than those deduced [3, 4] in the analysis of similar reactions taking place at 6-13 MeV/nucleon. Presumably this reflects the shorter time scale of the reactions at intermediate energies which does not allow rotation of the fissioning system prior to fission. The signs of the shift angles imply negative emission angles for the PLFs and are consistent with studies of γ-ray circular polarization in similar systems [17].

In Figure III-A-2a, we show the values of the deduced angular momentum transfer as a function of the linear momentum transferred to the fissioning nucleus for the reactions and Q value bins studied in this work along with all the available data for similar reactions leading to fissioning nuclei [8]. Figure III-A-2b contains similar data but for systems[6,7] in which the primary recoiling nucleus did not fission but formed an evaporation residue [16]. Although one could in general expect a correlation between angular momentum transfer and linear momentum transfer for a particular system [2, 6, 7], it is quite remarkable that there appears to be a universal correlation among these quantities in a wide variety of reacting systems. The generally higher values for the transferred angular momentum for a fissioning nucleus compared to one in which a residue is formed is qualitatively consistent with the expected lowering of the fission barrier with increasing angular momentum.

In Figure III-A-2c, we also show the universal behavior of the alignment P_{zz} of the transferred angular momentum (vs. the reaction Q value) for a series of low energy and intermediate energy reactions, [1, 3, 5] including this work. The qualitative trend of decreasing alignment with increasing energy transfer is consistent with excitation of randomly oriented thermal modes of the transition nucleus and/or the effects of increased pre-fission particle evaporation upon the alignment.

To understand the origin of these correlations, we have used two approaches, a microscopic and a macroscopic one. Starting from the perspective of low energy reaction mechanisms, we used the microscopic nucleon transport model of Randrup and Vandenbosch [18] to calculate the properties of the primary product nuclei prior to any de-excitation by fission or particle emission. (This model is an extension of transport calculations used to understand dissipation and the character of low-energy nuclear collisions ($E_{proj} < 10$ MeV/nucleon). We have calculated the transferred angular momentum as a function of the reaction Q value. From a detailed knowledge of the kinematics (O+Au) or the assumption of two body kinematics, we have transformed the Q values into values of P_R' with the results being shown in Figure III-A-2a and III-A-2b. The agreement between the measured and calculated values of $\ell_{transfer}$ is reasonable especially since no attempt was made to simulate the effects of spin fractionation during the de-excitation phase of the reactions. For the systems in Figure III-A-2a and III-2-b, the model predicts the observed correlation between $\ell_{transfer}$ and P_R'.

What is the physics involved in this correlation? The transferred angular momentum, L, is a double-valued function of the impact parameter, b. For central collisions in which there is complete overlap between the projectile and target nuclei, L increases with increasing b. For peripheral collisions an opposite trend occurs. The nucleon transport model indicates the observed approximate "universal" correlation only occurs for the "peripheral collision" regime. Surprisingly, a given L transfer occurs at an approximately constant b value for all the systems studied. In short, $L = b \times p$.

Carrying this simple macroscopic argument further, one can predict the "high energy limit" to this correlation. From the systematics of linear momentum transfer in relativistic nuclear collisions [19], we know that $\langle P_\parallel \rangle \approx (8\ MeV/c)\Delta A$, where $\Delta A = A_{target} - A_{fragment}$. Estimating that $\Delta A \approx |Q(MeV)|/10$ and assuming all high energy reactions take place in peripheral collisions ($b \approx 10$ fm), we can estimate that $\langle L\ (\hbar) \rangle \approx 0.04Q$. The present intermediate energy data lies systematically above the high energy limit (Figure III-2-a) and presumably reflects different mechanism(s) of linear and angular momentum transfer at intermediate and relativistic energies. If the corelation found in this work is universal, one can use either this correlation of the "high energy limit" to estimate the magnitude of the transferred angular momentum in peripheral collisions at intermediate or high energies, thus specifying one of the constants of motion of the nuclear system.

In summary, we have demonstrated the existence of an unexpectedly simple correlation between the transferred linear and angular momenta in intermediate energy collisions and between the alignment of the transferred angular momentum and the reaction Q value. The observed correlations are consistent with the nucleon transport model, suggesting the importance of deep inelastic processes as the dominant reaction mechanism in peripheral collisions at these energies.

(R. Yanez, W. Loveland, D.J. Morrissey, K. Aleklett, J.O. Liljenzin, E. Hagebo, D. Jerrestam, and L. Westerberg)

References

[1] P. Dyer, R.J. Puigh, R. Vandenbosch, T.D. Thomas, M.S. Zisman, and L. Nunnelley,

Nucl. Phys. **A322**, 205 (1979).
[2] G.J. Wozniak, C.C. Hsu, D.J. Morrissey, L.W. Richardson, and L.G. Moretto, LBL-13637, November, 1981.
[3] D.J. Morrissey, G.J. Wozniak, L.G. Sobotka, A.J. Pacheco, R.J. McDonald, C.C. Hsu and L.G. Moretto, Nucl. Phys. **A389**, 120 (1982).
[4] C. Le Brun, J.F. Lecolley, F. Lefebvres, M. L'Haridon, A. Osmont, J.P. Patry, J.C. Steckmeyer, and R. Chechik, Phys. Rev. **C25**, 3212 (1982).
[5] J.C. Steckmeyer, F. Lefebvres, C. Le Brun, J.F. Lecolley, M. L'Haridon, A. Osmont, and J.P. Patry, Nucl. Phys. **A427**, 357 (1985).
[6] M.N. Namboordiri, et al., Phys. Rev. **C35**, 149 (1987).
[7] K. Hagel, et al., Nucl. Phys. **A486**, 429 (1988).
[8] K. Ieki, et al., J. Phys. G. Nucl. Part. Phys. **18**, 401 (1992).
[9] See, for example, C. Gregoire and B. Tamain, Ann. Phys. Fr. **11323** (1986).
[10] B.B. Back, K.L. Wolf, A.C. Mignerey, C.K. Gelbke, T.C. Awes, H. Breuer, V.E. Viola, Jr., and P. Dyer, Phys. Rev. **C22**, 1927 (1980).
[11] A. Wieloch, et al. Nucl Phys. **A584,** 573 (1995).
[12] V.E. Viola, Jr., Nucl. Data Tables, **1**, 391 (1966).
[13] L.G. Moretto, and R.P. Schmitt, Phys. Rev. C21, 204 (1980); L.G. Moretto, S.K. Blau, and A.J. Pacheco, Nucl. Phys. **A364**, 125 (1981).
[14] R.A. Broglia, G. Pollarolo, C.H. Dasso, and T. Dossing, Phys. Rev. Lett. **43**, 1649 (1979).
[15] R.J. Puigh, P. Dyer, R. Vandenbosch, T.D. Thomas, L. Nunnelley, and M.S. Zisman, Phys. Lett. **86B**, 24 (1979).
[16] K. Aleklett, W. Loveland, T.T. Sugihara, A.N. Behkami, D.J. Morrissey, Li Wenzin, Wing Kot and G.T. Seaborg, Phys. Scripta **34**, 489 (1986).
[17] M.B. Tsang et al., Phys. Rev. Lett. **60**, 1479 (1988).
[18] J. Randrup, and R. Vandenbosch, Nucl. Phys. **A474**, 219 (1987).
[19] D.J. Morrissey, Phys. Rev. **C39**, 460 (1989).
[20] B.B. Back and S. Bjornholm, Nucl. Phys. **A302**, 343 (1978).
[21] A.J. Sierk, Phys. Rev. **C33**, 2039 (1986).
[22] R.P. Schmitt and A.J. Pacheco, Nucl. Phys. **A379**, 313 (1982).
[23] R. Yanez, et al. Oregon State University Nuclear Chemistry Progress Report 1995, p13.
[24] R. Yanez, et al. Phys. Lett. **B376**, 29 (1996).

TABLE I. Measured and Deduced Quantities for the Interaction 357 and 476 MeV ^{16}O with ^{197} Au.

Energy	Q(MeV)	K_0^2	$L_z(\hbar)$	χ(deg)	P_{zz}	P^{II}_R(GeV/c)
22	-130 ± 35	112	26.1 ± 2.6	4.0	0.70 ± 0.20	1.22 ± 0.23
	-205 ± 17	154	37.9 ± 2.0	11.8	0.69 ± 0.10	1.56 ± 0.11
	-249 ± 12	174	66.1 ± 5.2	-0.2	0.50 ± 0.11	1.74 ± 0.08
30	-191 ± 6	146	37.0 ± 4.4	-7.8	0.64 ± 0.21	1.25 ± 0.09
	-211 ± 6	156	40.8 ± 5.8	-10.1	0.60 ± 0.24	1.32 ± 0.10
	-230 ± 6	166	56.0 ± 6.3	-10.7	0.54 ± 0.20	1.42 ± 0.11
	-251 ± 6	174	42.3 ± 5.3	-3.9	0.58 ± 0.21	1.51 ± 0.10
	-270 ± 6	182	43.5 ± 5.0	-3.7	0.56 ± 0.18	1.58 ± 0.08
	-290 ± 6	190	47.0 ± 8.0	-3.3	0.49 ± 0.25	1.64 ± 0.06
	-310 ± 6	199	56.2 ± 13.1	-1.1	0.35 ± 0.28	1.71 ± 0.05
	-330 ± 6	204	63.1 ± 13.5	2.2	0.29 ± 0.24	1.81 ± 0.03

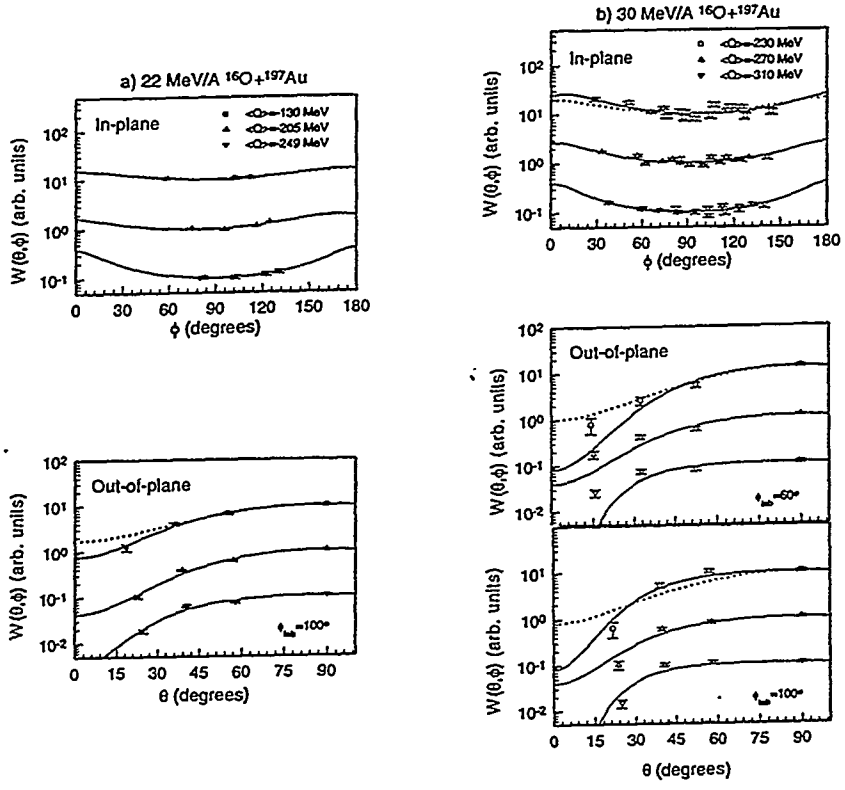

FIG. II-A-1. Measured in-plane and out-of-plane fission fragment angular distributions (in the frame of the fissioning nucleus) for the reaction of: (a) 357 MeV (22 MeV/nucleon) ^{16}O with ^{197}Au, and (b) 476 MeV (30 MeV/nucleon) ^{16}O with ^{197}Au. The solid lines represent the fitted values of the angular distributions using eq (2) and (3) while the dotted line represents the more exact calculation[20].

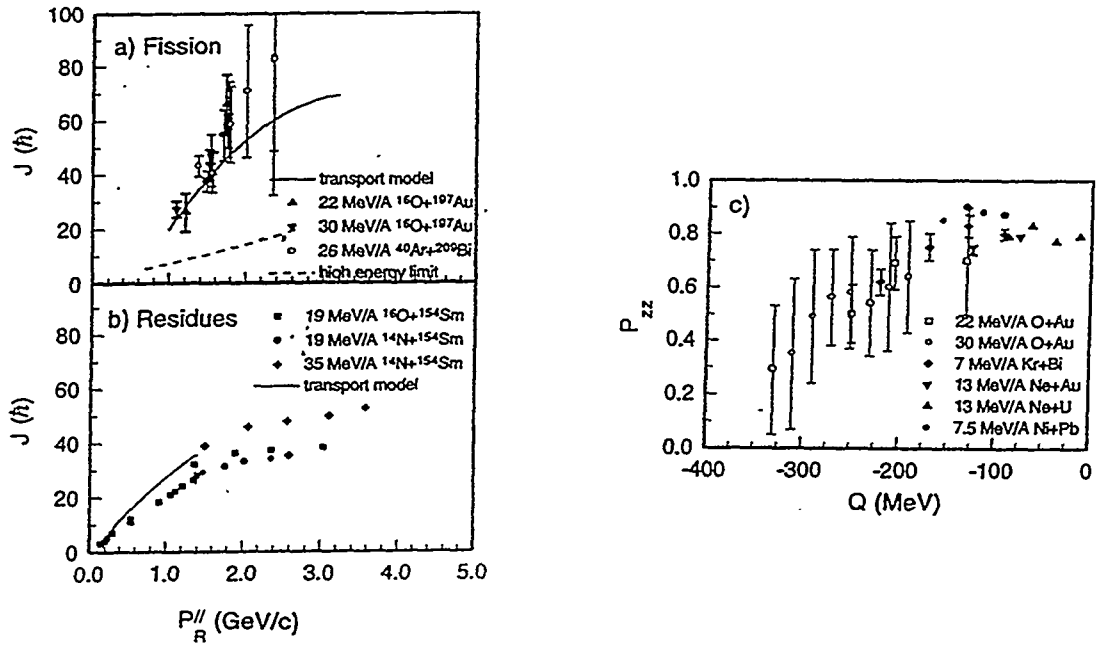

FIG.III-A-2. Systematics of transferred angular momentum vs. transferred linear momentum for: (a) fissioning nuclei, (b) residues, and (c) the alignment P_{zz} of the angular momentum as a function of the reaction Q value.

III.B Angular Momentum Transfer in the Reaction of 17 MeV/nucleon ^{40}Ar with ^{238}U

Recently we have completed the measurement of the in-plane and out-of-plane fission fragment angular distributions for the interaction of 22 and 30 MeV/nucleon ^{16}O with ^{297}Au using the cyclotron at the TSL[1]. From these measurements, we have deduced the correlated transferred linear and angular momenta and the alignment of the fissioning nucleus. Combining these data with the measurements of Ieki et al.[2] for the reaction of 26 MeV/nucleon ^{40}Ar + ^{209}Bi and the data of Namboodiri et al.[3] and Jacquet et al.[4] leads to a seemingly universal relationship between transferred linear and angular momentum for peripheral reactions for a wide variety of systems (Figure III-B-1).

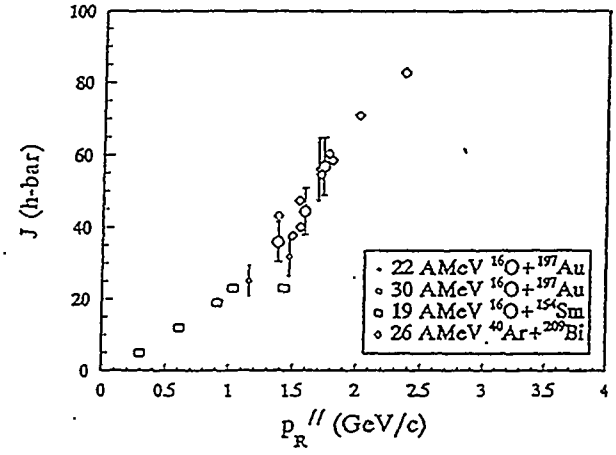

Figure III-B-1.Systematics of transferred angular and linear momenta for peripheral intermediate energy nuclear collisions.

While it is certainly not unexpected to see a correlation between transferred linear and angular momenta in a single reaction, to find such a correlation in data spanning a large range of reacting nuclei is unusual. These data offer the possibility of determining the partial waves associated with various reaction mechanisms, and thus leading to a more stringent test of various theoretical models of these collisions.

As experimentalists, we would like to test the rigor and universality of the apparent correlation seen in Figure 1. Accordingly we have undertaken the measurement of the linear and angular momentum transfer in the reaction of 17 MeV/nucleon ^{40}Ar with ^{238}U. The average spin transfer and its alignment will be deduced from in-plane and out-of-plane fission fragment angular distributions measured in coincidence with projectile-like fragments. The linear momentum transfer will be deduced by a simultaneous measurement of the fission folding angle distributions. The excitation energy of the fissioning system will be inferred from the asymmetry of the fission mass distributions measured in coincidence with projectile-like fragments.

We believe that such a measurement would have certain unique features when compared with previous studies: (a) the use of a very fissionable target nucleus, such as ^{238}U, instead of the less fissionable target nuclei used in previous studies will insure that all impact parameters and momentum transfers will lead to fission; (b) numerical simulations of this reaction using the microscopic nucleon transport model of Randrup and Vandenbosch[5] have been done (Figure III-B-2). Comparison of the measured data to these predictions can serve as a direct test of this model; (c) based upon FLMT systematics[6], the values of the transferred linear momenta (and thus the transferred angular

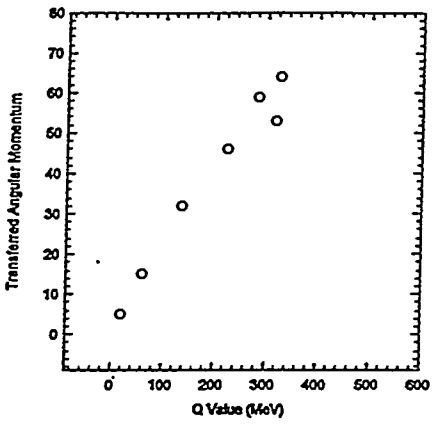

Figure III-B-2.Nucleon transport model calculations of the expected angular momentum transfer as a function of the Q value for the reaction of 17.3 MeV/nucleon ^{40}Ar with ^{238}U.

momenta according to Figure 1) should be similar for the O + Au and Ar + U reactions even though the expected reaction mechanisms should be different. This should furnish a stringent test of the robustness of the correlation; (d) the simultaneous measurement of linear momentum transfer and the Z of the projectile-like fragment along with the ℓ transfer and alignment should remove some model-dependent assumptions used in previous data analyses. For those events in which E* of the fissioning system can be inferred, an additional constraint is imposed; (e) all of the reactions should involve some fusion-like events which can be studied independently of the other events.

The experiment was performed at the GWI cyclotron at Uppsala. The experimental apparatus is shown in Figure III-B-3. Two multi-element Si detector telescopes for detecting the projectile-like fragments were located at the grazing angle. Fission fragment angular distributions were measured by a set of eight Si surface barrier detectors located on movable arms in and out of the reaction plane. From the fission fragment folding angle correlations, the linear momentum transfer to the fissioning nucleus was deduced. From the fragment angular distributions, the mean angular momentum transfer and its alignment was deduced, assuming a gaussian spin distribution in the fission system. From the fission-fission-PLF coincidences (in plane) one deduces the fragment mass distributions (E*) in coincidence with the Z of the PLF. Analysis of the data is underway.

[R. Yanez,J. Romanski, W. Loveland, K. Aleklett, J. O. Liljenzin, E. Hagebo, L. Westerberg]

References

1. R. Yanez, et al., Phys. Lett.
2. K. Ieki, et al., J. Phys. G.18, 401 (1992).
3. M. N. Namboodiri, et al., Phys. Rev. C35, 149 (1987).
4. D. Jacquet, et al., Nucl. Phys., A511, 195 (1990).
5. J. Randrup and R. Vandenbosch, Nucl. Phys. A474, 219 (1987).
6. B. Borderie and M. F. Rivet, Z. Phys. A321, 703 (1985).

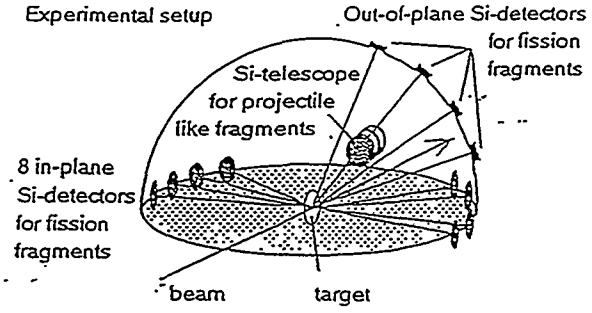

Figure III-B-3.Schematic diagram of experimental apparatus.

III C. High Resolution Studies of Heavy Residue Production in the Interaction of 20 MeV/nucleon ^{197}Au with ^{12}C and ^{27}Al

Recent measurements [1-3], utilizing inverse kinematics and high resolution magnetic spectrometers, have shown new and powerful ways of studying the formation of heavy residues in intermediate energy collisions. We have utilized these techniques to study the properties of heavy residues and fission fragments formed in the interaction of 20 MeV/nucleon ^{197}Au with ^{12}C, ^{27}Al and ^{nat}Ti.

The experiment was performed at MSU. A 20 MeV/nucleon ^{197}Au beam produced by the K1200 cyclotron, interacted with ^{12}C, ^{27}Al and ^{nat}Ti targets. The reaction products were analyzed using the A1200 mass separator and stopped in a three-element (50μm,50μm,and 300μm) Si surface barrier detector telescope (placed at the focal plane of the separator.) For each reaction product event, dE/d, E, time-of-flight and magnetic rigidity were measured. From these quantities, the product Z,A, q and velocity were calculated for each event. To cover a large range of fragments and their momentum distributions, a series of successive measurements at overlapping magnetic rigidity settings of the spectrometer were performed. For calibration of the Si telescope, low intensity beams of ^{197}Au, ^{129}Xe, ^{95}Mo, ^{54}Fe, ^{54}Cr and ^{27}Al at 20 MeV/nucleon were used. A detailed calibration of the Si detectors, taking into account the pulse-height defect (see section IV of this report), provided good energy-loss and total energy measurements. The average experimental resolution (FWHM) achieved during this experiment for the residues was 0.9 Z units, 0.9 q units, 1.5 a units and 0.8% for Z,q,A, and velocity, respectively. For fission fragments, the corresponding quantities were 0.6 Z units, 0.6 q units, 1.1 A units and 0.2%, respectively.

In Fig. III-C-1, contour plots of the isotopic cross sections in the Z versus A plane for the ^{197}Au + ^{12}C, ^{27}Al reactions are shown. The distributions of the heavy residues peak at the neutron-deficient side of the valley of nuclear stability and extend to lower masses as the mass of the target increases. These distributions extend to the limits of nuclear stability (towards the proton drip-line) and may contain new very neutron-deficient nuclei. In contrast to the heavy residues, the distributions of the fission fragments, peak close to the valley of nuclear stability. The difference between the distributions with the Al and C targets is indicative of the different reaction mechanisms operating (see below).

In Fig. III-C-2, the isobaric yield distributions for these reactions are shown. The shapes of these distributions are generally similar to those obtained by radiochemical measurements of target-like fragments from similar reactions at this energy range [4,5]. In Figure III-C-3 we show some typical charge distributions for the Au + Al reaction. One notes the rather complete character of these distributions, with up to 12 points spanning two or more orders of magnitude. (This is to be compared to typical radiochemical work where 2-4 points are measured per A value). The shapes of the measured distributions are Gaussian vindicating a frequently-made, but unverified assumption.

In Figure III-C-4, we show the mass-resolved product velocity distributions . One can clearly identify peaks for quasi-eleastic and fusion-like events in the residue distributions. The

fractional linear momentum transfer for the fusion-like events is 0.80 and 0.83 for the Au + C,Al reactions, in agreement with FLMT systematics. Cross sections of 300 and 80 mb are found for the fusion-like residues for the Au + C,Al reactions with cross sections for fusionlike-fission events being 1600 and 2500 mb. The peripheral collison cross sections are 500 and 1600 mb for the Au+C, Al reactions.

One additional feature of the A-resolved velocity distributions (such as Fig. III-C-4) worthy of note is that the residue mass number is not an impact parameter trigger, as it is in higher energy collisions. One can observe, for a given mass number, a range of residue velocities (transferred momenta) which indicate a range of impact parameters. This feature is consistent with BUU calculations [6] of residue properties in similar systems at somewhat higher energies.

One can gain further insight into the impact parameter dependence of residue formation using the residue velocities to sort the data. To define a velocity scale that can be related to impact parameter in a simple way, the velocities of the residues were transformed in the moving frame of the projectile and were expressed as a fraction of the complete-fusion velocity (in the projectile frame). (In this definition of fractional velocity , v_R/v_{CF}, commonly used in normal kinematics , complete fusion corresponds to v_R/v_{CF} =1, and peripheral collisions to v_R/v_{CF}=0.)

The two-dimensional Z vs. A distributions of the heavy residues were generated for five velocity intervals spanning the range of v_R/v_{CF} from 0.0 to 1.0. Subsequently, for each fractional velocity window, the isobaric yield distributions (Fig. II-C-5) were created and, the isobaric Z distributions of the residues were generated and their centroids and standard deviations were obtained. A cursory examination of the data shown in Figure III-C-5 shows expected trends. As the transferred momentum increases, the excitation energy of the primary residues increases, leading to neutron emission that produces observed residues that are more neutron deficient. The widths of the secondary residue charge distributions also generally increase with increasing excitation energy of the residue precursor. Where comparisons are made for the Au + C reaction, the radiochemical measurements appear to be in acceptable agreement with this work although the assignment of events as fusion-like or quasielastic in that work was arbitrary.

A very interesting feature of the fusion-like products (v_R/v_{CF} ~ 0.80) is the presence of heavy residues very close in charge and mass to the compound nucleus ^{209}At (E^*≈ 208 MeV). These products have appreciable yields and are not due to tails of the yields of lower mass residues due to the resolution of the spectrometer. Similar products have been observed in a recent radiochemical study of the reaction of 10 MeV/nucleon C+Au and were satisfactorily described by means of a Boltzmann master equation approach.

Comparison of the velocity-resolved data from the Au + C and Au + Al reactions shows a number of differences between the two reactions. In the Au + Al reaction, as the transferred momentum (residue velocity) increases, the average mass number of the surviving residue shifts to lower values while in the Au + C reaction, the average residue mass is relatively insensitive to the transferred linear momentum. The widths of the charge distributions are generally larger for most velocity bins for the Au + Al reaction compared to the Au + C reaction, except for the fusion-like collision bin where the reverse is true.

In this experiment, an incomplete scan of the fission fragment distributions was made.

However, it is interesting to see what we might learn from studying the heavy fragment distributions we have. We first verified that the fission fragments originated in fusion-like events with an average FLMT of 0.8-0.9. We then examined the N/Z dependence of the heavy fission fragment yields.

An important parameter that characterizes the fission process is the division of nuclear charge between two fragments. Such charge distributions are frequently parameterized as having a Gaussian form

$$Y(Z)=\frac{1}{(2\pi)^{1/2}\sigma_Z}\exp[\frac{-(Z-Z_p)^2}{2\sigma_Z^2}]$$

where σ_Z is the Gaussian width parameter and Z_p is the most probable primary fragment atomic number for a given isobaric series. In charge equilibration at fixed mass number, the N/Z mode is commonly described [7,8] as a harmonic oscillator having a phonon energy $\hbar\omega$ with the charge variance being described as

$$\langle\sigma_Z^2\rangle=\frac{1}{M\omega^2}(0.5\hbar\omega+\frac{\hbar\omega}{e^{\hbar\omega/T}-1})$$

where M is the inertia parameter of the N/Z mode and T is the temperature.
At low temperatures typical of thermal neutron induced fission, this equation becomes

$$\langle\sigma_Z^2\rangle=\frac{\hbar}{2M\omega}$$

Data for thermal neutron-induced fission [9] agree with this prescription and $\langle\sigma_Z^2\rangle$can thus be described as a result of the zero point oscillations of a harmonic oscillator in the charge equilibration mode. At higher temperatures, this equation becomes

$$\langle\sigma_Z^2\rangle=\frac{T}{M\omega^2}$$

In model-independent language, the variance of the fission charge distribution is a function of the isospin correlations in the nuclear ground state and their behaviour with increasing temperature.

The fission fragment charge distributions are shown in Figure III-C-6. As found in the radiochemical studies [5], all yields can be plotted on a single Gaussian curve with the best fit value of the variance, $\langle\sigma_Z^2\rangle$ being 1.2 . If we assume [7] that the phonon energy of the deformed fissioning system is given as

$$\hbar\omega\sim\frac{78}{A_1^{1/3}+A_2^{1/3}}(MeV)$$

and that the stiffness $M\omega^2$ is given as

$$M\omega^2=1.39(A_1^{-1/3}+A_2^{-1/3})+186.28(\frac{1}{A_1}+\frac{1}{A_2})-\frac{2.88}{1.24(A_1^{1/3}+A_2^{1/3})}$$

we can calculate expected values of $\langle\sigma_Z^2\rangle$ for these two systems. The results of that calculation (Figure III-C-7) indicate the observed variance of the charge distributions exceeds that expected using a model of a time dependent harmonic oscillator in the charge equilibration mode. Such observations have been seen at lower temperatures, but this observation represents one of the first observations for a well-characterized system at higher temperatures.

The large cross sections associated with the formation of residues (which decay by particle emission or fission) indicate that the reaction processes under study are very important components of the overall reaction. The results of this high resolution study should be an important testing ground for phenomenological models of intermediate energy collisions. The "low" projectile energy of 20 MeV/nucleon should emphasize the "mean field" aspects of these collisons and thus, test this component of the models.

In our initial attempt to understand this data, we have used three different models. The first of these is a schematic model of incomplete fusion (ICF) [10] which essentially models the reaction as a fusion of a piece of the target, picked to reproduce the average FLMT, with the projectile. The model assumes binary collision dynamics and leads to a predicted primary distribution of nuclei with a mean Z,A,E*,v and a 2J+1 distribution of J values.

The second model chosen for study was the nucleon transport model [11]. This model is an extension of transport calculations used to understand dissipative processes in low energy collisions.

The third model used was the numerical implementation of the BUU model developed by Bauer [12]. We have assumed a soft equation of state (K=200) and followed the evolution of the collisions for b=0...14 fm in 1.0 fm steps for times of 0 to 200 fm/c in steps of 5 fm/c, using 75 test particles per nucleon. At a time of 120 fm/c we stopped the BUU calculation and calculated the values of Z,A,J,E*,and v of the targetlike residue.

The de-excitation of the primary residue distribution predicted by each of these models was calculated using a modified version of PACE[13]. A temperature-dependent value of a was used [14] and a_f/a_n was set equal to 1.00 [15].

The results of the calculations for the Au+C,Al reactions are compared to the data in Figures III-C-8 and III-C-9. These calculations are evaluated on how well the models reproduce the fission/residue yield ratio, the position in the Z,A plane of the predicted residue distribution and the mean velocity of the residues for fusion-like events.

The ICF model correctly predicts the mean residue velocity for fusion-like events by design, and does a reasonable job of predicting the fission/residue cross section ratio. The predicted residue distributions are in rough accord with the mean Z and A of the fusion-like residues, but, of course, do not resemble the yields from more peripheral collisions. The success of this "model" also indicates the approximate correctness of the de-excitation calculation using PACE.

The predictions of the nucleon transport model differ significantly from the observations. The predicted fission/residue ratio is too low, and the locus of the predicted residue distribution in the (Z,A) plane is too neutron-deficient and is peaked at too low a mass number. These deficiencies can be traced back to a lack of appreciable mass transfer in the model from target to projectile is this asymmetric collision. The primary products after the initial interaction are close to the projectile and as a consequence, have reduced fissionability and result in products of lower mass number upon de-excitation.

Calculations using the BUU model are in progress.

(G.A. Souliotis,, W. Loveland, K. Hanold, I. Lhenry, G.J. Wozniak, D.J. Morrissey, and A.C. Veeck)

References

[1] D. Bazin et al., Nucl. Phys. **A515**, 349 (1990).
[2] B. Faure-Ramstein, et al., Nucl. Phys. **A586**, 533 (1995).
[3] K. Hanold, et al., Phys. Rev. **C52**, 1462 (1995).
[4] W. Loveland et al., Phys. Rev., **C41**, 973 (1990).
[5] H. Kudo, K.J. Moody and G.T. Seaborg, Phys. Rev., **C30**, 1561 (1984).
[6] M.B. Tsang, et al., Phys. Rev. **C40**, 1685 (1989).
[7] M. Berlanger, et al., Z. Phys. **A291**, 137 (1979).
[8] H. Nifenecker, J. Phys. (Paris) Lett. **41**, L-47 (1980).
[9] J.P. Bocquet, and R. Brissot, Nucl. Phys. **A502**, 213c (1989).
[10] N. Colonna, et al., Phys. Rev. Lett. **62**,1833 (1989).
[11] J. Randrup and R. Vandenbosch, Nucl. Phys. A474, 219 (1987).
[12] W. Bauer, Phys. Rev. **C40**, 715 (1989)
[13] A. Gavron, in **Computational Nuclear Physics 2: Nuclear Reactions**, K. Langanke, J.A. Maruhn, and s.E. Koonin, eds. (Springer-Verlag, New York, 1993), p 108.
[14] S. Schlomo and J. B. Natowitz, Phys. Rev. **C44**, 2878 (1991).
[15] Th. Rubehn, K.X. Jing, L.G. Moretto, L. Phair, K. Tso, and G.J. Wozniak, LBNL-38865.

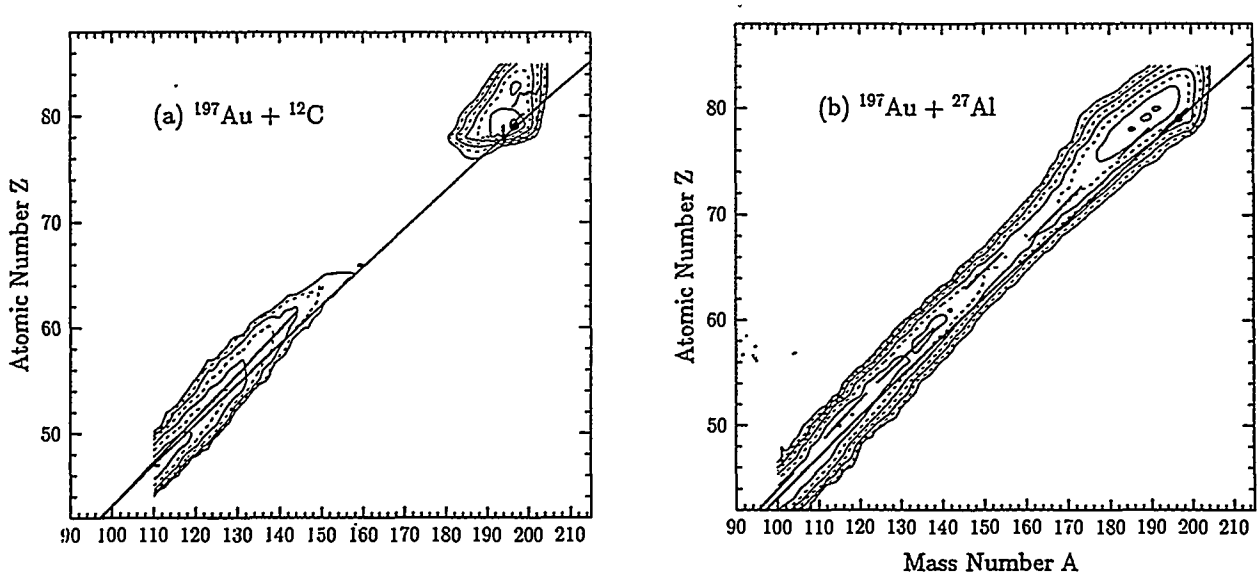

Figure III-C-1 Contour plots of the reaction product yields from the interaction of 20 MeV/nucleon ^{197}Au with ^{12}C and ^{27}Al. The line of β-stability is indicated as a continuous solid line while the short line segments indicate the position of the most probable atomic number Z_p found in radiochemical studies[5].

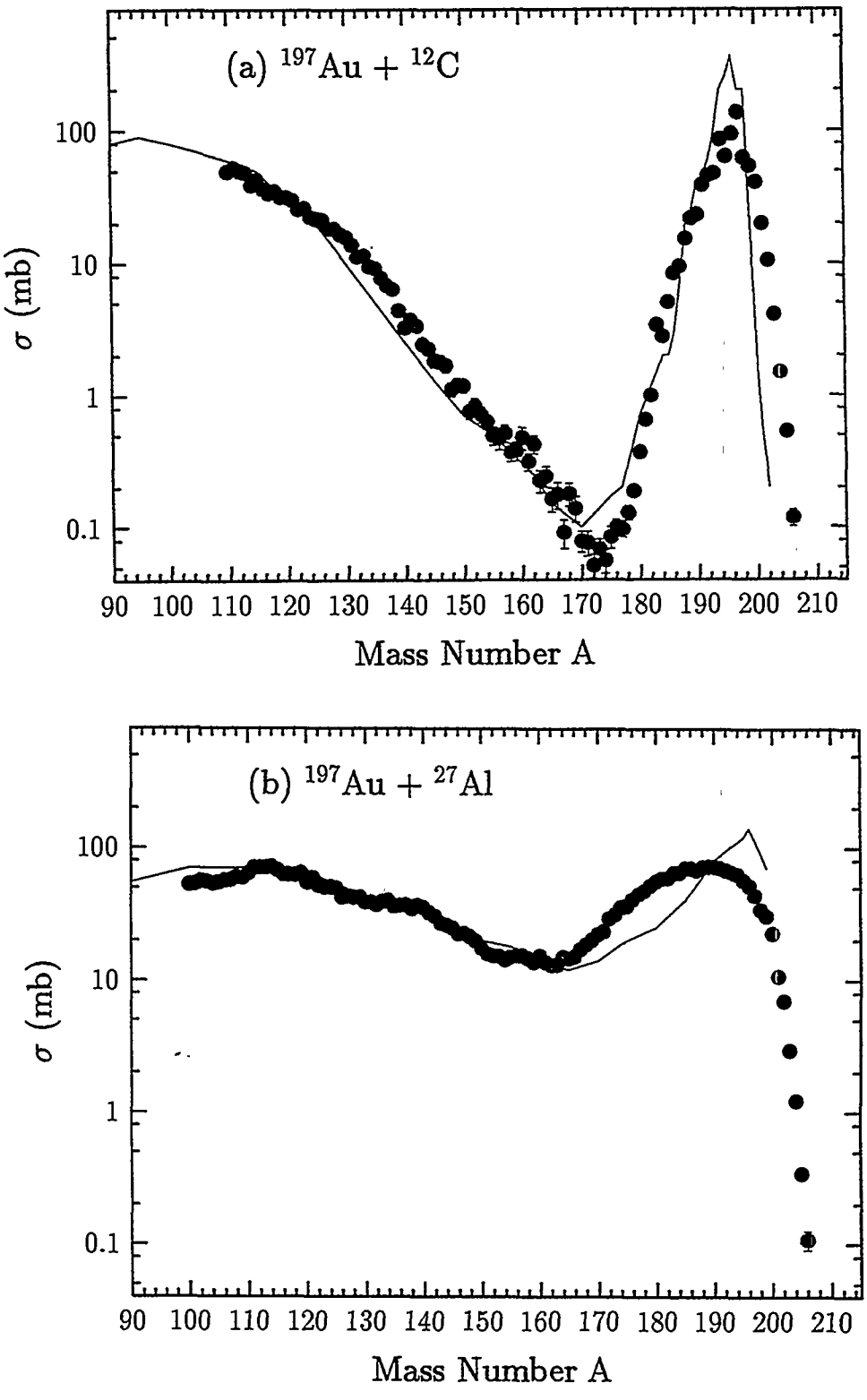

Figure III-C-2 Isobaric yield distributions for the 20 MeV/nucleon ^{197}Au + ^{12}C,^{27}Al reactions. The solid lines indicate the radiochemical data [4,5] for the ^{12}C + ^{197}Au and ^{32}S + ^{197}Au reactions at 20 and 17 MeV/nucleon, respectively.

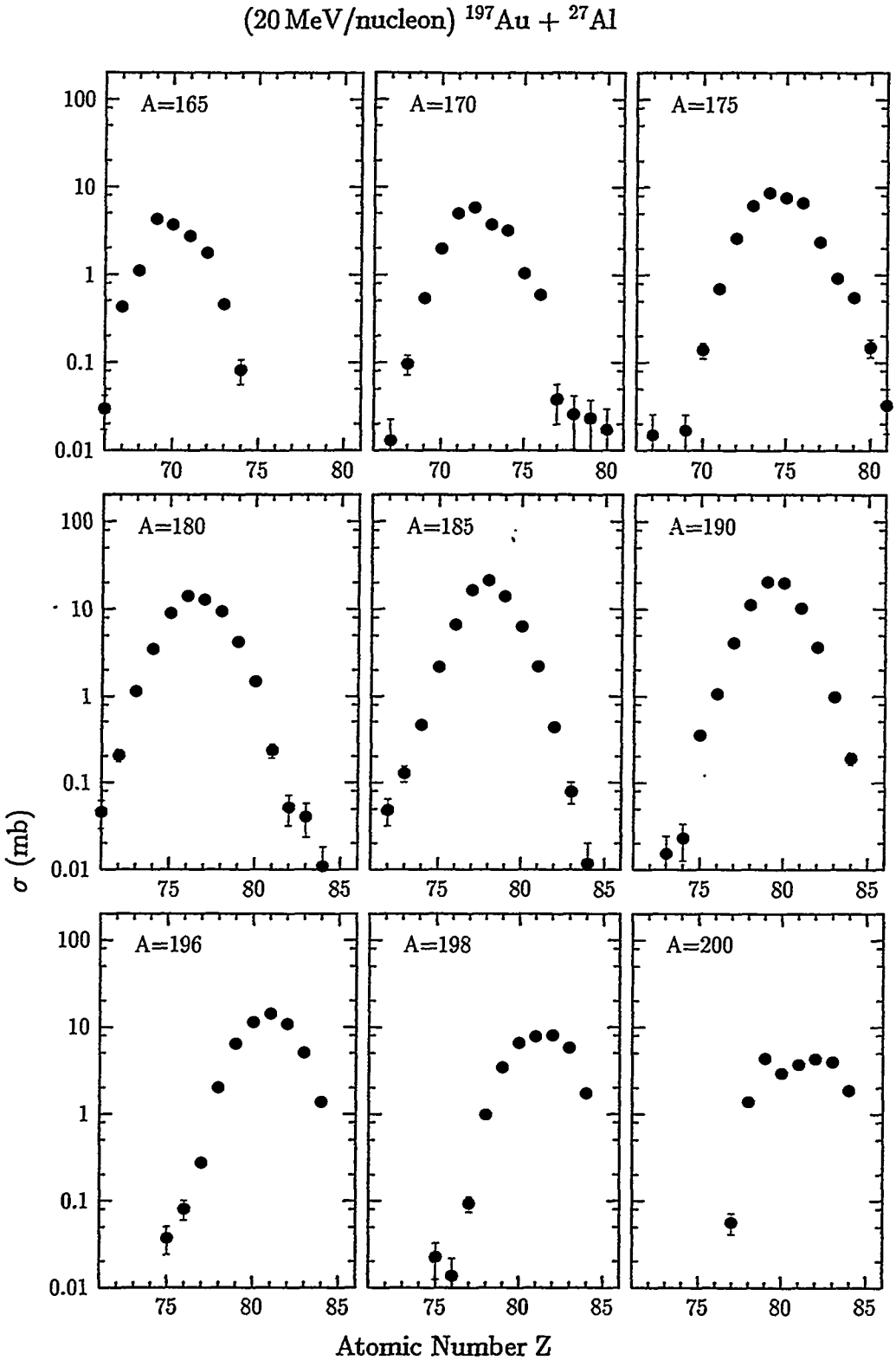

Figure III-C-3. Heavy residue charge distributions for the 20 MeV/nucleon ^{197}Au + ^{27}Al reaction.

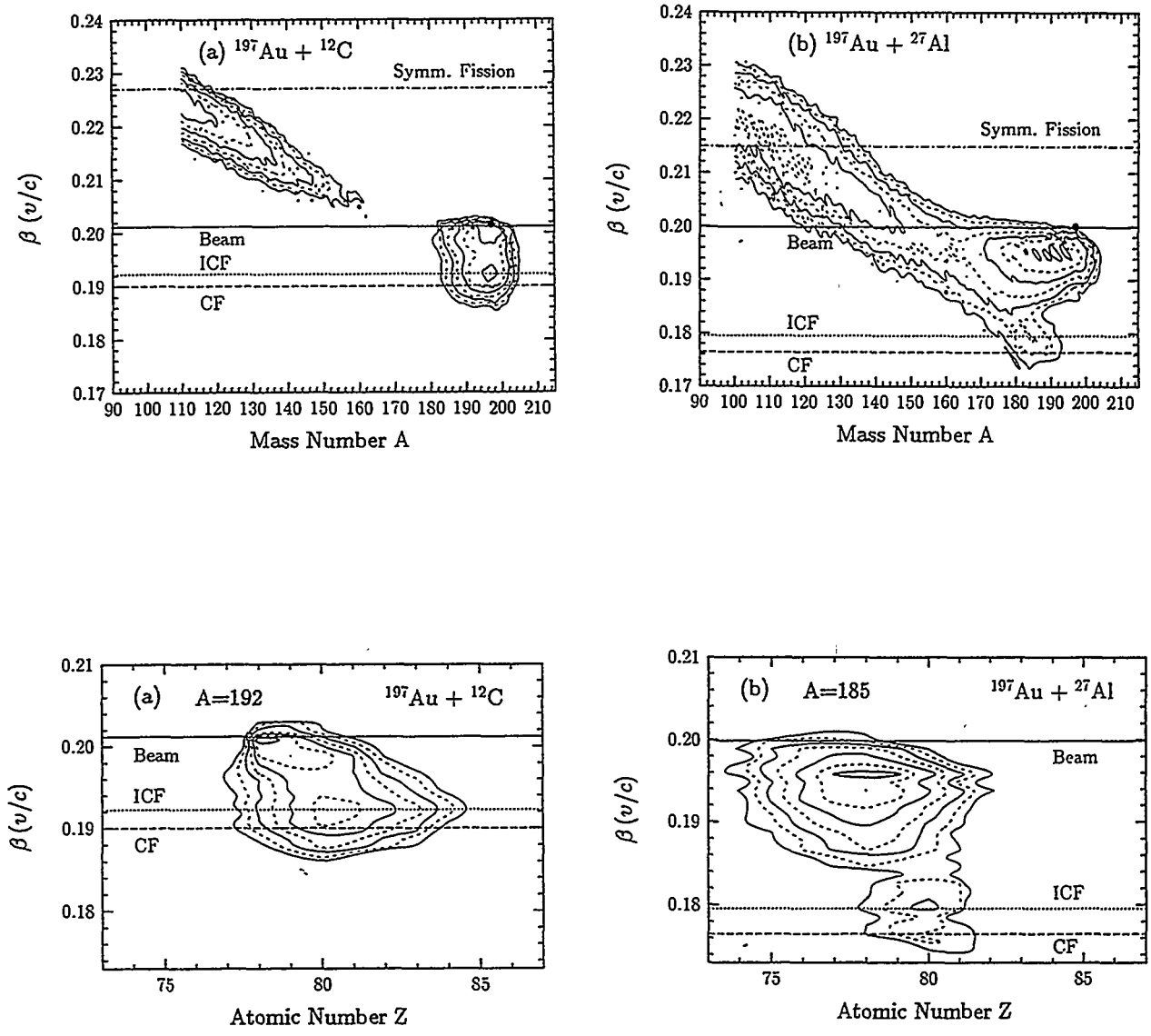

Figure III-C-4. Mass resolved velocity distributions for the Au + C,Al reactions.

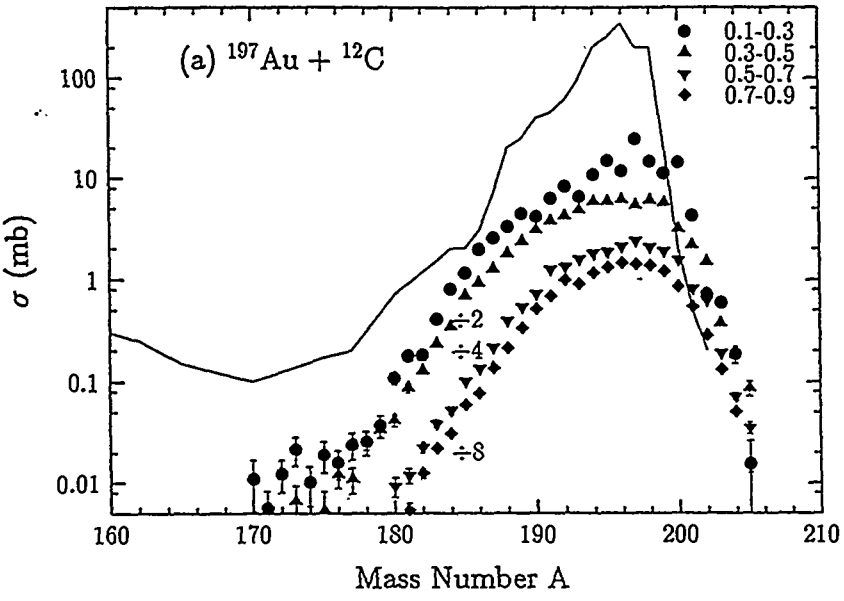

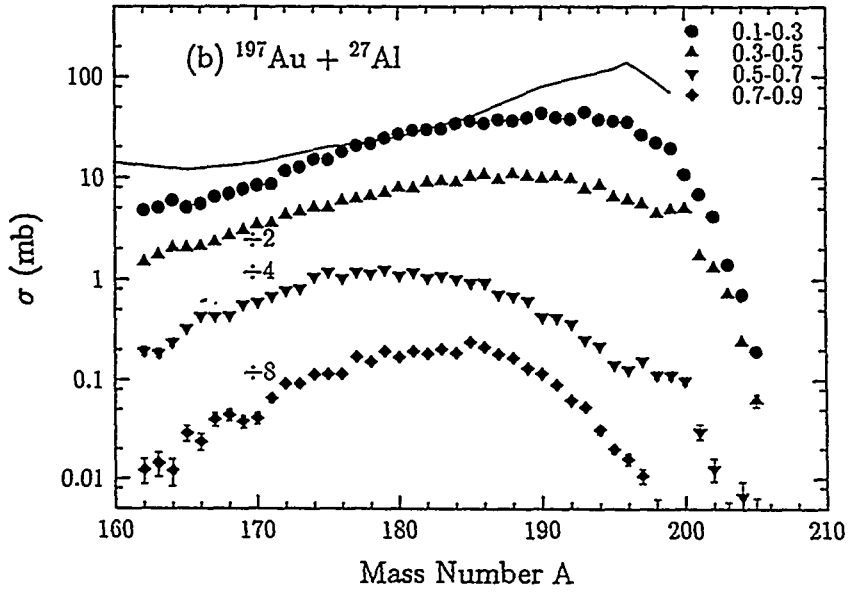

Figure III-C-5 Velocity sorted residue distributions.

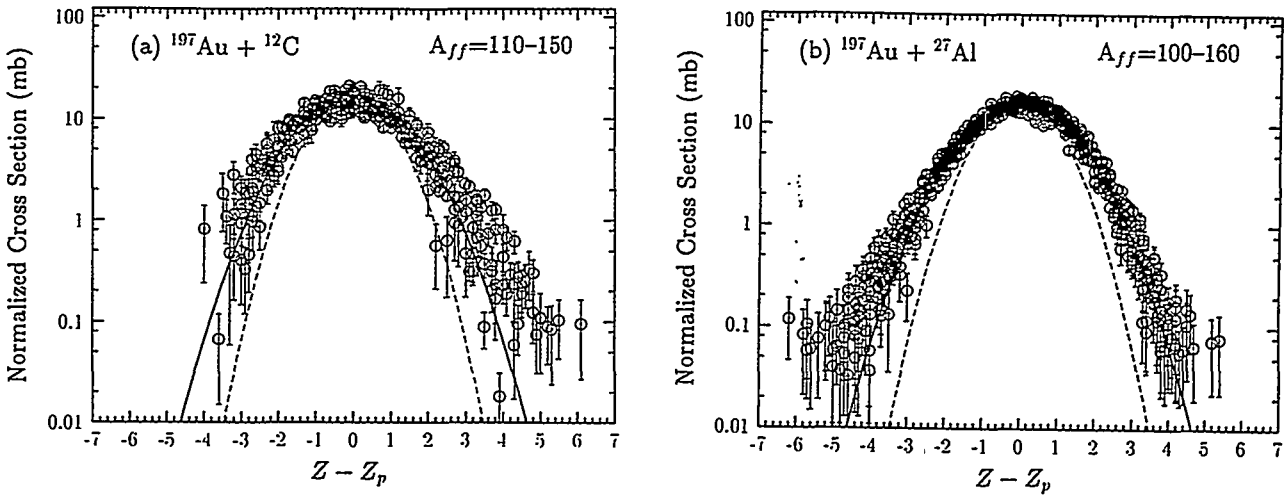

Figure III-C-6 Fission fragment charge distributions for the Au +C,Al reactions.The solid lines indicate the fitted charge distribution (wider curve) and that expected from the thermal model (narrower curve).

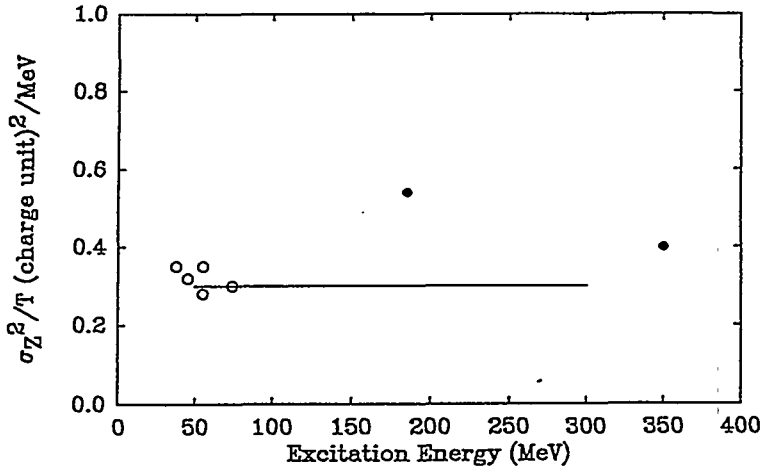

Figure III-C-7 Temperature dependence of the variance of the fission charge distributions. The solid line indicates the prediction of the thermal model.

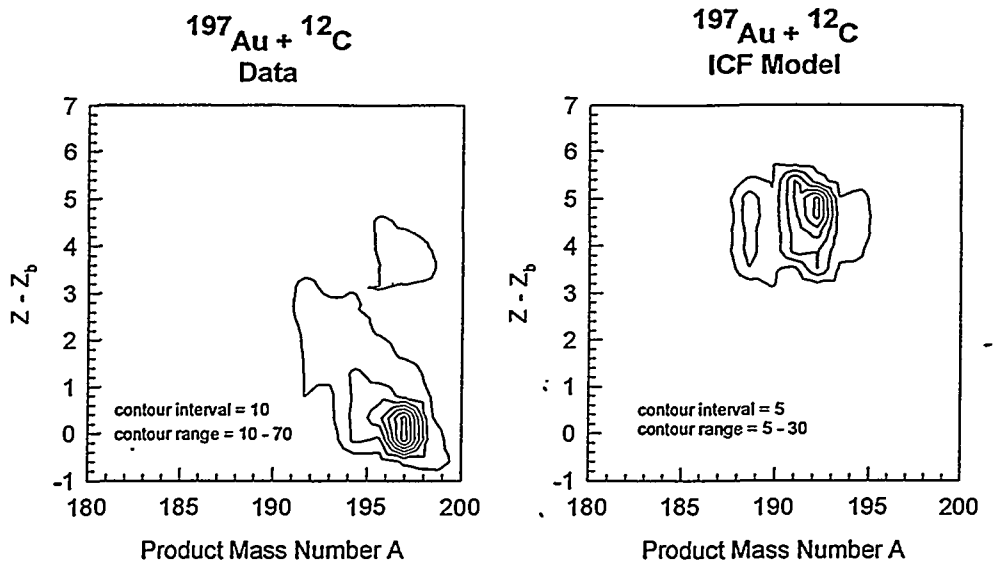

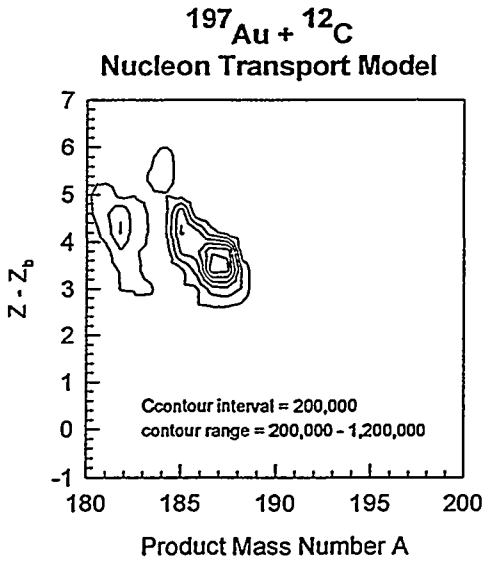

Table of Residue Properties

20 MeV/nucleon ^{197}Au + ^{12}C

	data	ICF	Nucleon transport
residue survival probability	16%	13%	78%
v_R/v_{CF}	0.80	0.80	0.73

Figure III-C-8. Comparison of measured and predicted residue properties for the 20 MeV/nucleon ^{197}Au + ^{12}C reaction. The peak at Z-Z$_\beta$ =0 is due to quasi elastic scattering while the fusion-like residues are at Z-Z$_\beta$ ≈4.

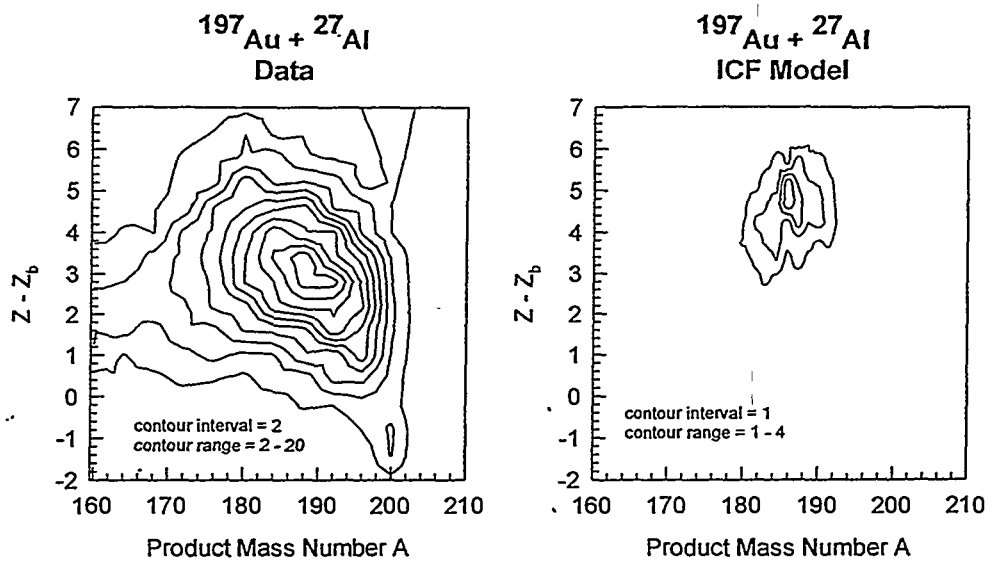

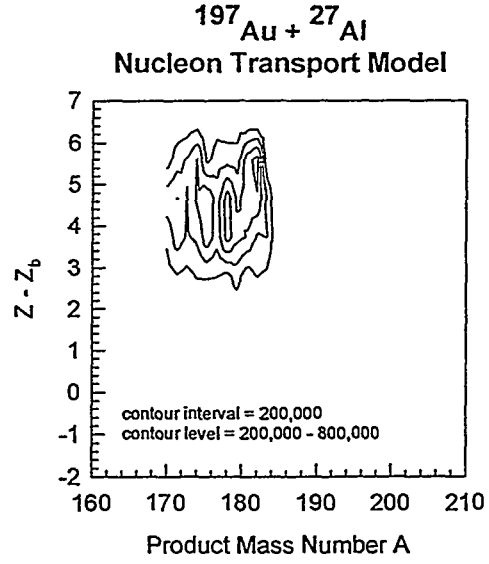

Table of Residue Properties

20 MeV/nucleon $^{197}Au + ^{27}Al$

	data	ICF	Nucleon transport
residue survival probability	3.1%	2.9%	34%
v_R/v_{CF}	0.83	0.83	0.75

Figure III-C-9. Comparison of measured and predicted reasidue properties for the 20 MeV/nucleon $^{197}Au + ^{27}Al$ reaction.

III-D. Heavy Residue Properties in the Interaction of 20 MeV/nucleon ^{197}Au with ^{nat}Ti, ^{90}Zr, and ^{197}Au: Generation of New Nuclides and Radioactive Beams

Studies of the interaction of 20 MeV/nucleon ^{197}Au with ^{12}C and ^{27}Al (see section III-C) have shown significant differences in heavy residue yields and properties with the two target nuclei. In going from ^{12}C to ^{27}Al, a sharp decrease (300 mb → 80 mb) occurs across in the fission-like events with a corresponding increase in dissipative phenomena. Since we had anticipated such a result, we also studied the interaction of 20 MeV/nucleon ^{197}Au with ^{nat}Ti at the same time as the Au + C, Al studies.

The experimental conditions were the same as described in Section III-C. The MSU A1200 fragment separator/detector system was used to measure the Z, A, velocity and yield of the residues. (The ^{nat}Ti target thickness was 2.3 mg/cm^2.) Due to limits on accelerator time, the Bρ settings used for the measurements only allowed the detection of the residues (A>150) and no fission fragments.

The heavy residue isobaric yield distribution, nuclidic yield distribution, selected charge distributions and velocity-resolved residue distributions are shown in Figures III-D-1 – III-D-4. The experimental resolution is the same as in the Au + C,Al study. If these distributions are compared to the corresponding ones from the 20 MeV/nucleon ^{197}Au + ^{12}C, ^{27}Al reaction (Figures III-C-1--III-C-4), one notes several substantive differences. The isobaric yield distribution shows a simple exponential decrease in yield as one goes to smaller A values starting from the target mass number. This decrease is characteristic of what one expects[1] from a highly excited system, formed by dissipation of the kinetic energy of the projectile into internal energy of the residue precursor. The velocity distribution shows an absence of fusion-like events with most collisions resulting in small (~20%) linear momentum transfer. The charge distributions are much broader than those seen in relativistic nuclear collisions[1], but are **identical** to those seen in the Au + Al reaction. Since the variance of these distributions at high excitation energy is proportional to the nuclear temperatures, this finding implies a constant temperature of the residue precursors in these reactions.

One notes that the charge distributions observed in the Au + Al, Ti reactions are substantially broader than those expected from relativistic nuclear collisions (Figure III-D-3). One also notes the yields of n-deficient nuclides are substantially greater in the projectile fragmentation cases. Some of the nuclides shown in Figure III-D-3 are "unknown".

In Figure III-D-5, we show a portion of the Chart of the Nuclides with an indication of the positions of the nuclides seen in the "first" Au + Ti experiment. **In our distributions of the yields of residues of a given Z and A, we have significant numbers (5-100) of counts for Z, A pairs that correspond to 48 new nuclides[3].** We also know this is a lower limit on the number of new neutron deficient nuclides as the spectrometer momentum scans and the data analysis to-date has cut off fragments with Z≥85 although there is evidence (Figure III-D-2) of the possible existence of more n-deficient nuclides with Z≥85.

The question is whether one can claim the identification of a new nuclide when the A1200 spectrometer resolution (FWHM) was 0.9 Z units, 0.9 q units, and 1.5 A units. Simulations indicated that most of these "nuclides" (counts in a given Z, A bin) were not the tails of more abundantly produced nuclides closer to stability. Nonetheless, we felt that an additional

experiment with improved resolution was indicated. In January, 1996, we re-measured with improved resolution the heavy residue yields as a function of Z, A and velocity for the interaction of 20 MeV/nucleon ^{197}Au with ^{9}Be, ^{12}C, ^{48}Ti, ^{90}Zr and ^{197}Au. The new resolutions (FWHM) are 0.9 Z units, 0.6 q units and 1.0 A unit for the heavy residues and 0.6 Z units, 0.5 q units and 0.7 A units for the fission fragments. While the analysis of these data is on-going, first results have confirmed the production of several new nuclides.

One is driven to ask the possible significance of these new nuclides for the generation of beams of radioactive nuclei for the study of nuclei far from stability. In Table III-D-1, we show the "bench mark facility" intensities[2] for some n-deficient A=185 nuclides produced in an ISOL facility with those expected from the proposed MSU coupled cyclotron facility operated as a PF radioactive beam facility. Although it might seem the PF facility beams are lower in intensity than those expected from the ISOL facility, one must also include the release efficiencies in the ISOL estimates (which have not been included in ref [2]). With that perspective in mind, it would appear that fragmentation of heavy beams can offer a useful alternative in producing radioactive beams of n-deficient heavy nuclei.

[G. A Souliotis, W. Loveland, K. Hanold, G. J. Wozniak]

References

1. K. Sümmerer et al., Phys. Rev. C42, 2546 (1990).
2. The Isospin Laboratory, LALP-91-51.
3. Table of Isotopes, Eighth Edition, R. B. Firestone, V. S. Shirley, ed. (Wiley, New York, 1996).

Table III-D-1
Yields of A=185 Radioactive Beams (part/s)

	Po	Bi	Pb
ISOL facility[2] (100 μA, 1000 MeV protons incident on 250 g/cm^2 UC)	4.8×10^4	2.9×10^6	2.8×10^7
MSU coupled cyclotron (10 pna, 100 MeV/A ^{197}Au incident on 100 mg/cm^2 Ti)	8×10^3	8×10^4	3.2×10^5

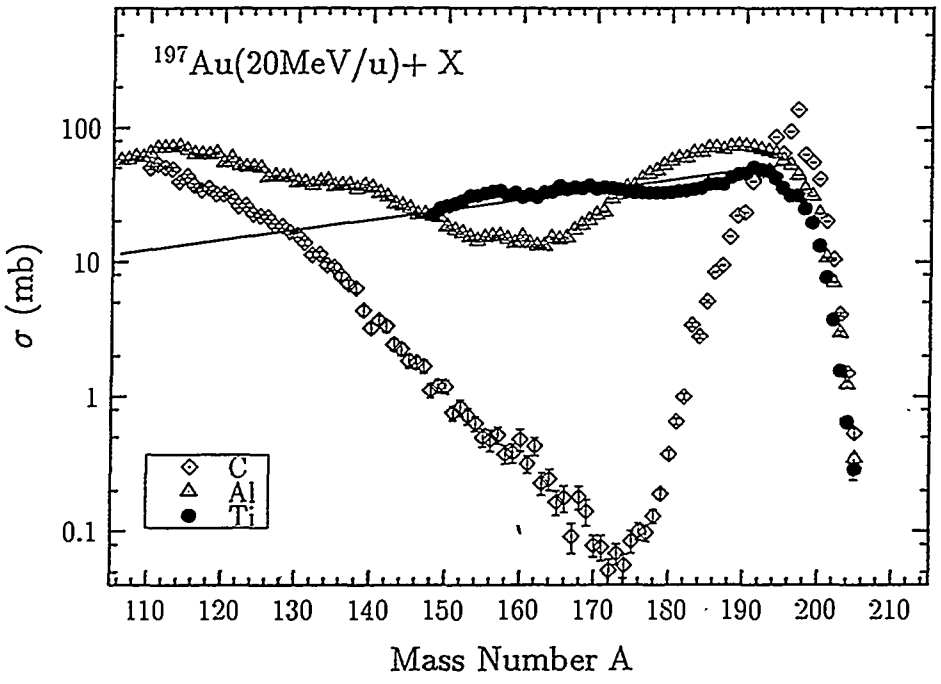

Figure III-D-1. Isobaric yield distribution for the reaction of 20 MeV/nucleon ^{197}Au with C,Al, and Ti. The solid line indicates the mass-yield curve expected [1] for relativistic nuclear collisions.

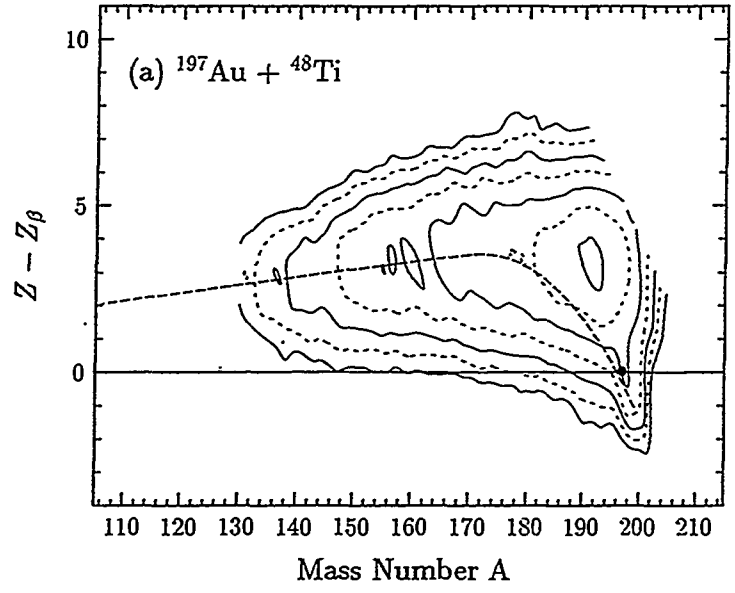

Figure III-D-2.The yields of individual residue nuclei displayed as contours of $Z-Z_\beta$ vs mass number A. (Z_β is the line of β- stability.) The Z_p (A) dependence in relativistic collisions [1] is shown as a dashed line.

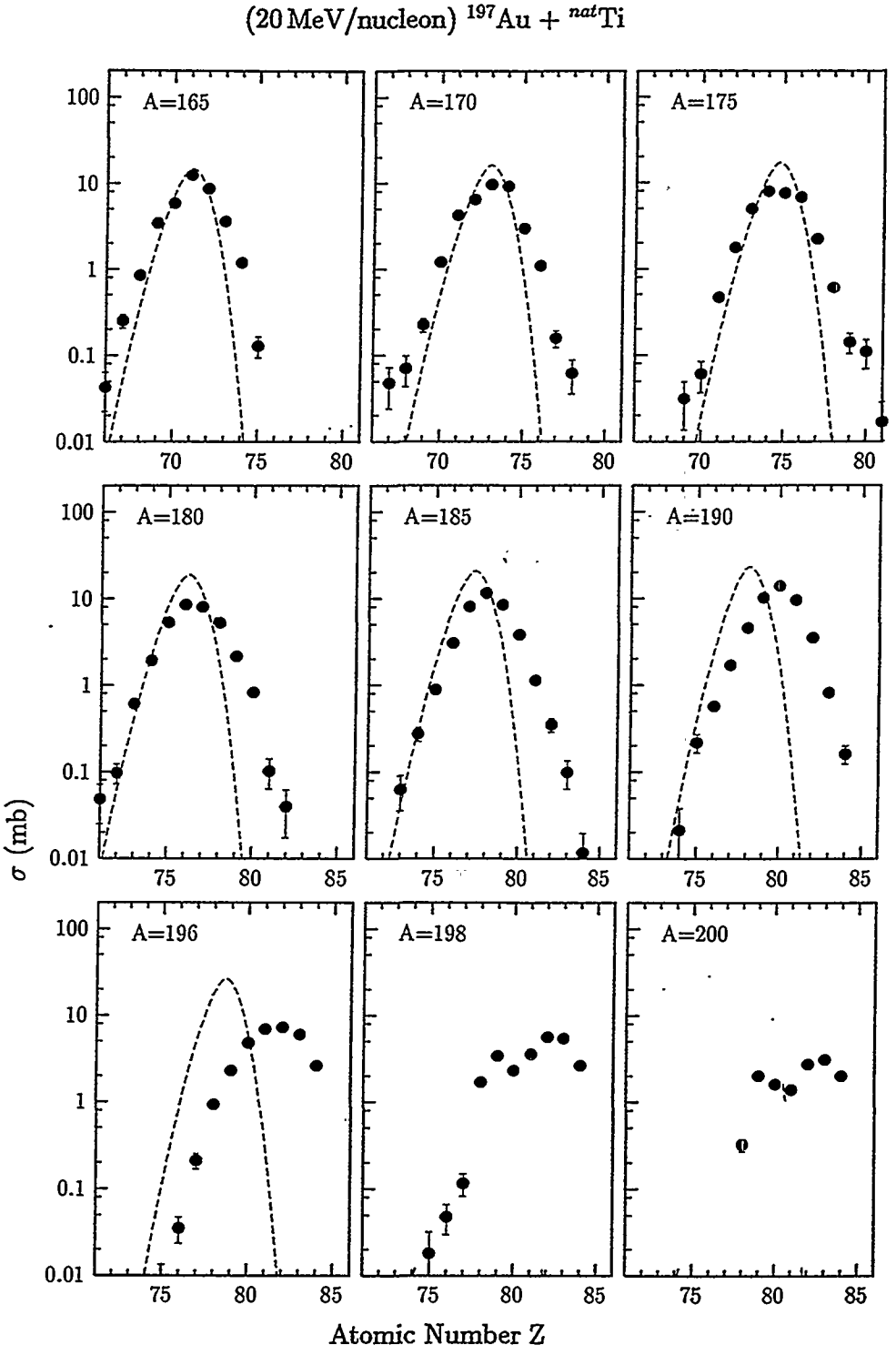

Figure III-D-3.Representative nuclidic charge distributions for the ^{197}Au + ^{nat}Ti reaction. The dashed curves are those expected[1] for relativistic nuclear collisions.

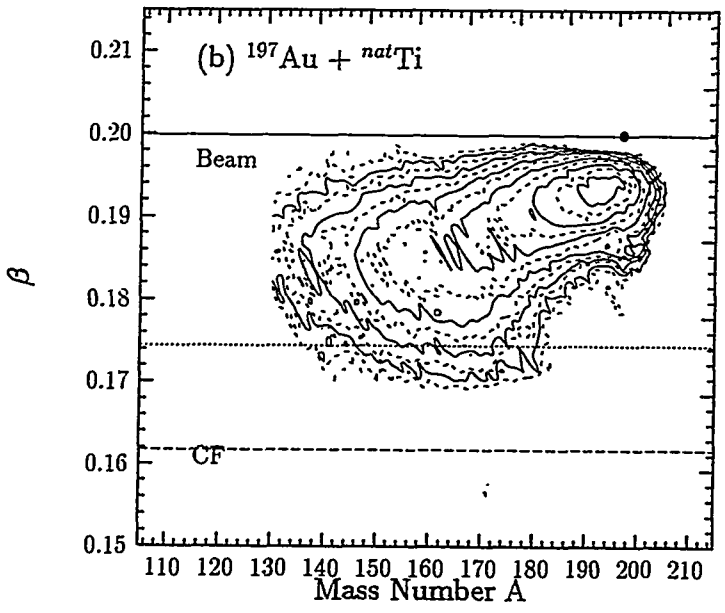

Figure III-D-4. Velocity (β=v/c) resolved residue yields for the ^{197}Au + ^{nat}Ti reaction. The velocity of the beam (solid line) and a completely fused system (dashed line) are shown.

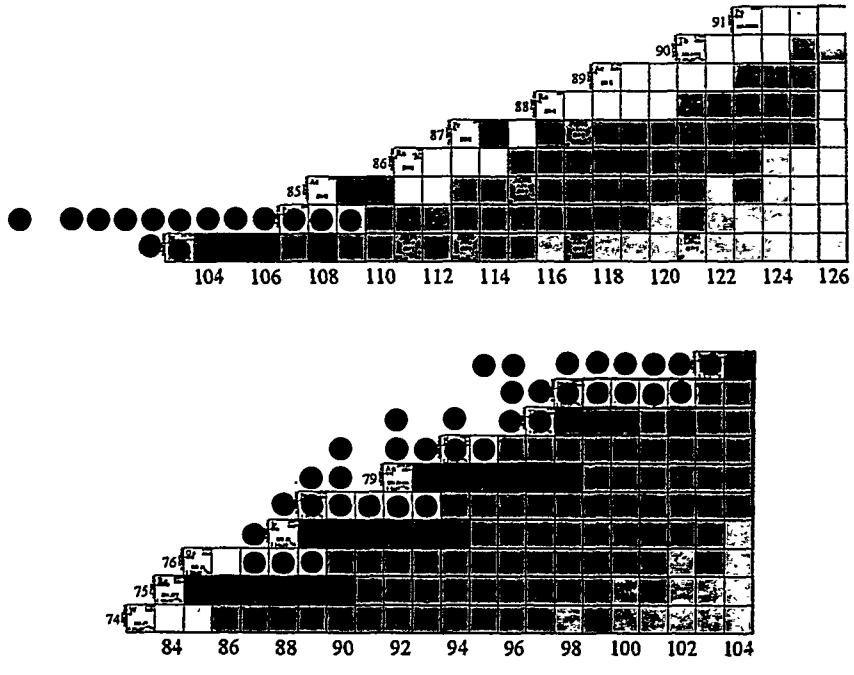

Figure III-D-5. A portion of the Chart of Nuclides where the "●" symbol indicates the new radionuclides formed in the reaction of 20 MeV/nucleon ^{197}Au with ^{nat}Ti.

.III-E. Heavy Residue Properties in Dissipative $^{86}Kr + ^{197}Au$ Collisions at 35 MeV/nucleon

Spurred on by observations [1, 2] of the importance of binary dissipative collisions in intermediate energy reactions, the Rochester/St. Louis groups performed an exclusive study of heavy residue formation in a reaction, 35 MeV/nucleon $^{86}Kr + ^{197}Au$, where dissipative phenomena might be expected to be important. The exclusive study involved the use of the Rochester Super Ball to detect neutrons, the St. Louis Microball to detect light charged particles, and IMF, Si telescopes to detect PLFs and Si strip detectors to detect heavy residues. Because of our previous radiochemical studies [3, 4] of this heavy residue production reaction, we assisted in this April, 1994 experiment.

Two reports of the results of this experiment concerning heavy residues have been submitted for publication [5, 6]. Among the findings were the following:

(a) a deflection function for the system that looked very similar to the Wilczynski plots for low energy collisions was observed, indicating the occurrence of a dissipative orbiting process. The associated particle multiplicities increased as one followed along the trajectory of increasing dissipation.

(b) two classes of "heavy residues" were observed, corresponding to sequential fission fragments and the "true" heavy residues, i.e., the slow-moving large (A>140) fragments of the target nucleus.

(c) the association of large dissipation with the production of heavy residues relative to fission fragments (Figure III-F-1), i.e., heavy residue formation becomes favored over fission with increasing excitation energy [4].

(d) the occurrence of intermediate mass fragment emission also represses fission as a de-excitation mechanism [7].

(W. Skulski, B. Djerroud, D. K. Agnihotri, S. P. Baldwin, W. U. Schröder, J. Tôke, X. Zhao, L. G. Sobotka, R. J. Charity, J. Dempsey, D. G. Sarantities, B. Lott, W. Loveland, K. Aleklett)

References

[1] B. Lott, et al., Phys. Rev. Lett. **68**, 3141 (1992).
[2] S. P. Baldwin, et al., in Proc. 9th Winter Workshop on Nuclear Dynamics, Key West, World Scientific, Singapore (1993), p. 36.
[3] K. Aleklett, et al., Phys. Lett. **B236**, 404 (1990).
[4] W. Loveland, et al., Phys. Rev. **C41**, 973 (1990).
[5] W. Skulski, et al., Phys. Rev. **C53**, R2594 (1996).
[6] B. Djerroud, et al., Proc. 12th Winter Workshop on Nuclear Dynamics, Snowbird, Utah, February, 1996.
[7] R. Yanez, et al., Phys. Rev. **C52**, 203 (1995).

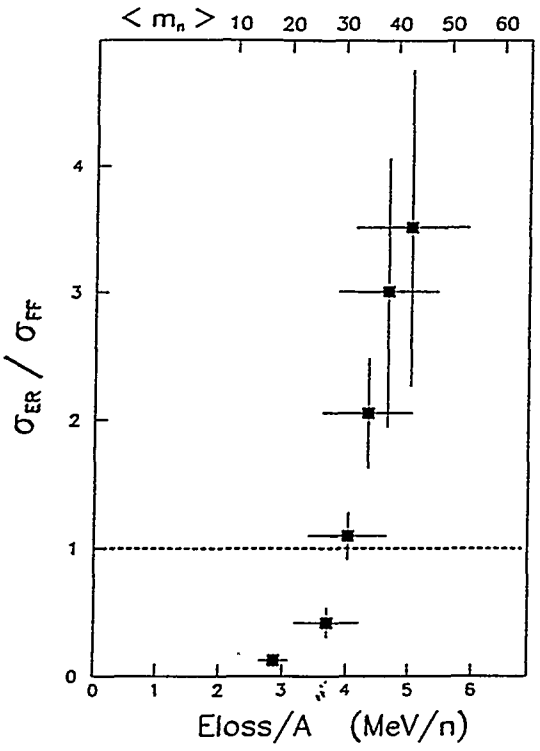

Figure III-F-1.Evolution of the intensity ratio σ_{ER}/σ_{FF} as a function of the total energy loss per nucleon. For a given energy loss, the associated average multiplicity of neutron is shown on the top of the figure.

IV. Technical Developments

IV-A. Pulse Height Defects for Very Heavy Ions

As part of the measurement of the energies of heavy residues using semiconductor detectors one must make significant corrections for the "pulse height defect" associated with their detection. The pulse height defect (PHD), which is generally defined as the difference between the true energy E_t and the apparent energy E_a measured with the detector, is due to three sources. These are the window defect ΔE_w, the nuclear stopping defect ΔE_n, and the residual defect ΔE_r. The window defect is due to the loss of energy of the ion upon passing the front electrical contact and the insensitive Si dead layer beneath it before reaching the depletion region. The nuclear stopping defect arises because the ions will partly slow down through non-ionizing nuclear collisions rather than ionizing electronic collisions in the detector material. The residual defect is thus $\Delta E_r = \Delta E - \Delta E_w - \Delta E_n$ and is usually interpreted as the loss of charge carriers due to trapping and recombination centers in the silicon crystal.

During the work outlined in this report and previous reports, we have measured the pulse height defect for very heavy ions of energies ranging from keV/nucleon to several MeV/nucleon in a number of detectors. Although we did not attempt a systematic study of these phenomena

because there is some lack of a coherent source of information about pulse height defects for these nuclei, we thought it might be useful to summarize our findings. We find that:

(a)the pulse height defects for nuclei with Z>50 are quite large, ranging from 15 MeV (for 100 MeV ^{209}Bi ions) [1] to 250 MeV for 1400 MeV ^{197}Au ions [2]. Neglect of this phenomenon is generally not justified.

(b)the pulse height defect is an "end of range" phenomenon, presumably due to the residual defect. No pulse height defect was observed for 20 MeV/nucleon ^{197}Au impinging on several 50μ - 100μ transmission detectors, but was observed in the stopping of the same ions on other parts of the detector telescope [2].

(c)the observed pulse height defects for a given heavy ion can differ in two detectors cut from the same piece of Si operated in exactly the same manner [Figure IV-A-1].

(d)None of the current prescriptions for pulse height defect will adequately predict the observed defect. The prescription of Moulton et al. [3] appears to have the correct functional form but must be adjusted for each detector. (Figure IV-A-2)

(e)Given (c) and (d) above, it is essential to use calibration beams to measure the pulse height defect in all measurements of the energies of very heavy ions using semiconductor detectors.

A related observation is that of an "avalanching" or "breakdown" discharge in 50μ ORTEC transmission mounted surface barrier detectors when 20 MeV/nucleon ^{197}Au or ^{238}U interacts with a detector operating at its recommended (overbiased) voltage (electric field $E_g = 6.5 \times 10^3$ V/cm). Reducing the operating voltage to retain the depletion depth, but reducing the electric field to $E_g = 3 \times 10^3$ V/cm caused the problems to disappear.

(G.A. Souliotis, R. Yanez and W. Loveland)

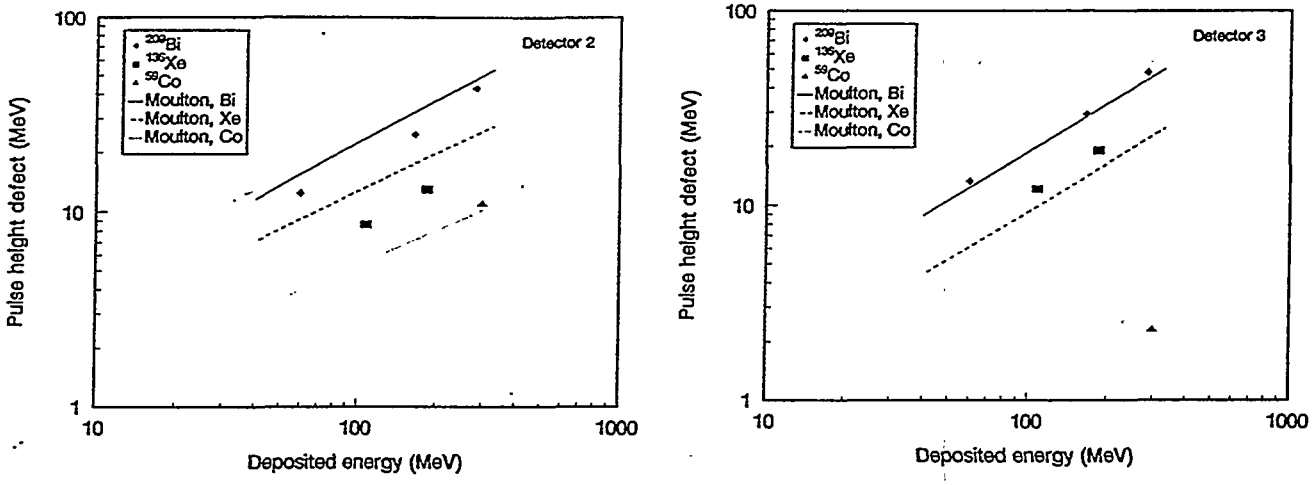

Figure IV-A-1.Response of two identical 450 mm^2, 100μ ORTEC surface barrier detectors to monoenergetic Xe and Bi ions.

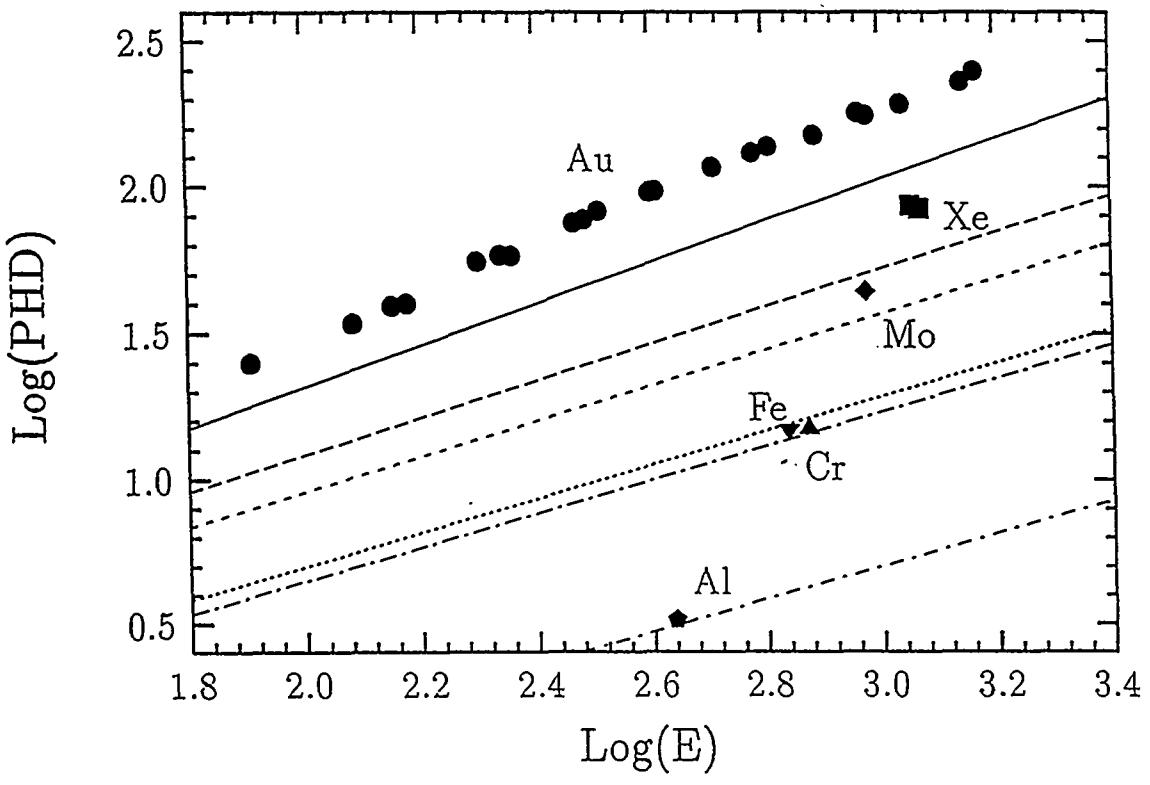

Figure IV-A-2.Deposited energy vs. pulse height for energetic very heavy ions intersecting with a surface barrier detector. The filled circles indicate the response to Au ions while the other symbols refer to other ions. The various lines represent the prediction of Moulton's formula

References

1. W. Loveland, R. Yanez, J. O. Liljenzin, K. Aleklett and A. Ghiorso, "The Pulse Height Defect of heavy Ions in Surface Barrier Detectors", Studsvik Neutron Research Lab Report NFL-77 (1995).
2. G. A. Souliotis, et al., Section III-C of this report.
3. J. B. Moulton, J. E. Stephenson, R. P. Schmitt, and G. J. Wozniak, Nucl. Instr. Meth. 157, 325

V. Personnel

Walter Loveland ..... Professor of Chemistry
George Souliotis ..... Postdoctoral Research Associate
Travis Day ..... Graduate Research Assistant
John Dunn ..... Graduate Research Assistant

Kristiana E. Zyromski ..... Graduate Research Assistant
Ida Forsberg ..... Visiting Scientist, Sweden
Brian Leen ..... ASE Summer Student
Nathaniel Grier ..... ASE Summer Student

During the past year, we have had the privilege of collaborating with a number of scientists from other institutions. The following list summarizes the names of many of these individuals (and their home institutions) who contributed to work described in this report.

D. K. Agnithotri (Rochester)
K. Aleklett (Uppsala)
S. P. Baldwin (Rochester)
O. Batenkov (Khlopin Radium Institute)
R. J. Charity (Washington Univ.)
J. Dempsey (Washington Univ.)
B. Djerrond (Rochester)
E. Hagebø (Oslo)
K. Hanold (LBL)
D. Jerrestam (Uppsala)
I. Lhenry (LBL)
J. O. Liljenzin (Chalmers)
B. Lott (GANIL)
L. G. Moretto (LBL)
D. J. Morrissey (MSU)
C. Powell (MSU)
D. G. Sarantities(Washington Univ.)
W. U. Schröder (Rochester)
W. Skulski (Rochester)
L. G. Sobotka (Washington Univ.)
J. Töke (Rochester)
A. Veeck (LBL)
L. Westerberg (Uppsala)
G. J. Wozniak (LBL)
X. Zhao (Rochester)

VI. Publications

A. Articles in Print

1. "Radioactivity," W. Loveland, in Encyclopedia of Applied Physics, G.L. Trigg, Ed. (VCH Publishers, New York, 1996), Vol 15, pp547-563.
2. "Systematics of Angular Momentum Transfer in Intermediate Energy Nuclear Collisions," R. Yanez, W. Loveland, D.J. Morrissey, K. Aleklett, J.O. Liljenzin, E. Hagebø, D. Jerrestam and L. Westerberg, Phys. Lett.**B376**, 29 (1996).

3. "Origin of slow heavy residues observed in dissipative $^{197}Au + ^{86}Kr$ collisions at E/A = 35 MeV," W. Skulski, B. Djerrond, D.K. Agnithotri, S.P. Baldwin,, J. Töke, X. Zhao,W.U. Schröder, L.G. Sobotka, R.J. Charity, J. Dempsey, D.G. Sarantities, B. Lott, W. Loveland and K. Aleklett, Phys. Rev. **C53**, R2594 (1996).

B. Articles Submitted /Accepted For Publication

1. "The Search for New Elements," W. Loveland and G.T. Seaborg, in The New Chemistry, N. Hall, Ed. (Cambridge).

2. "Possible Synthesis of Element 110 and the Future Prospects for Superheavy Elements," W. Loveland, Proc. 11th Winter Workshop on Nuclear Dynamics.

3. "Heavy Residue Production in Dissipative $^{197}Au + ^{86}Kr$ Collisions at E/A = 35 MeV," W. Skulski, B. Djerrond, D.K. Agnithotri, S.P. Baldwin, W.U. Schröder, J. Töke, X. Zhao, L.G. Sobotka, R.J. Charity, J. Dempsey, D.G. Sarantities, B. Lott, W. Loveland and K. Aleklett, Proc. 11th Winter Workshop on Nuclear Dynamics.

4. "Nuclear Chemistry with Accelerators," W. Loveland, in Frontiers in Nuclear Chemistry, D.D. Sood, Ed.

5. "Fusion Enhancement with Neutron-Rich Radioactive Beams", K.E. Zyromski, W. Loveland. G.A. Souliotis, D.J. Morrissey, C.F. Powell, O. Batenkov, K. Aleklett, R. Yanez,and M. Sanchez-Vega, Phys. Rev. Lett.

6. "Incomplete Energy Damping and Heavy Residue Production in $^{197}Au + ^{86}Kr$ Collisions at E/A= 35 MeV", B. Djerroud, W. Skulski, D.K. Agnihotri, S.P. Baldwin, W.U. Schroeder, J. Toke, L.G. Sobotka, R.J. Charity, J. Dempsey, D.G. Sarantities, B. Lott, W. Loveland, and K. Aleklett, Proc. 12th Winter Workshop on Nuclear Dynamics, Snowbird, Utah

7. "Heavy Residue Production in the Interaction of 29 MeV/nucleon ^{208}Pb with ^{197}Au ", W. Loveland, M. Andersson, K.E. Zyromski, N. Ham, B. Altschul, J. Vlcakova, J.O. Liljenzin, R. Yanez, and K. Aleklett, Phys. Rev. C.

C. Oral Presentations

1. "Systematics of Angular Momentum Transfer in Intermediate Energy Nuclear Collisions," K. Aleklett, R. Yanez, W. Loveland, D.J. Morrissey, J.O. Liljenzin, E. Hagebø, D. Jerrestam and L. Westerberg, INPC '95, Beijing, China, August, 1995.

2. "Evidence for the Possible Synthesis of Element 110," A. Ghiorso, D. Lee, L.P.

Somerville, W. Loveland, J.M. Nitschke, W. Ghiorso, G.T. Seaborg, P. Wilmarth, R. Leres, A. Wydler, M. Nurmia, and K. Gregorich, INPC '95, Beijing, China, August, 1995.

3. "Heavy Residue Production in Ar-Th Collisions at 44, 77 and 95 MeV/A," W. Loveland, R. Yanez, K. Aleklett, A. Srivastava and J.O. Liljenzin, INPC '95, Beijing, China, August, 1995.

4. " Fusion Enhancement with Neutron-Rich Projectiles", W. Loveland, Michigan State University, E. Lansing, MI, August, 1995.

5. "Fusion Enhancement with Neutron-Rich Projectiles", W. Loveland, PacChem'95, Honolulu, Hawaii, December, 1995.

6. " Systematics of Angular Momentum Transfer in Intermediate Energy Nuclear Collisions,", W. Loveland, R. Yanez, K. Aleklett, D.J. Morrissey, J.O. Liljenzin, E. Hagebo, D. Jerrestam, and L. Westerberg, PacChem'95, Honolulu, Hawaii, December, 1995.

7. "High Resolution Studies of Heavy Residues from ^{197}Au Fragmentation at 20 MeV/nucleon", G.A. Souliotis, K. Hanold, W. Loveland, M. Hellstrom, I. Lhenry, D.J. Morrissey, A.C. Veeck, and G.J. Wozniak, 51st ACS Northwest Regional Meeting, June, 1996.

8. "Fusion Enhancement with Neutron-Rich Radioactive Beams", K.E. Zyromski, W.D. Loveland, G.A. Souliotis, D.J. Morrissey, C. Powell, K. Aleklett, R. Yanez, M. Sanchez-Vega, and O. Batenkov, 51st ACS Northwest Regional Meeting, June, 1996.

9. " Incomplete Energy Damping and Heavy Residue Production in ^{197}Au+^{86}Kr Collisions at E/A=35 MeV", B. Djerroud, W. Skulski, D.K. Agnihotri, S.P. Baldwin, J. Toke, W.U. Schroeder, L.G. Sobotka, R.J. Charity, J. Dempsey, D.G. Sarantities, B. Lott, W. Loveland, and K. Aleklett, 12th Winter Workshop on Nuclear Dynamics, Snowbird, Utah, February, 1996.

Appendices removed

At the request of the Richland Operations Office of the U.S. Department of Energy, we have included copies of reprints and preprints (not previously submitted) corresponding to work performed during this period as part of the Annual Progress Report.